NUMERICAL ANALYSIS
of
OF NONLINEAR EQUATIONS

Kyoto, July 2006

Eusebius Doedel

Introduction

First we consider some simple examples of nonlinear equations, in order to motivate the numerical methods discussed later.

Persistence of Solutions

If
$$G \; : \; \mathrm{R}^n \; \times \; \mathrm{R}^n \; \to \; \mathrm{R}^n \; ,$$

with
$$G(u_0, \lambda_0) \; = \; 0 \; ,$$

and if
$$G_u(u_0, \lambda_0)^{-1} \;\; \text{exists} \; ,$$

then u_0 is said to be an *isolated solution* of $G(u, \lambda_0) \; = \; 0$.

The IFT (Implicit Function Theorem) states that isolation (plus Lipschitz continuity assumptions) implies the existence of a locally unique *solution family* (or *solution branch*)

$$u \; = \; u(\lambda) \; , \qquad u(\lambda_0) \; = \; u_0 \; .$$

Example: a Predator-Prey Model

$$
\begin{cases}
u_1' &= \quad 3u_1(1 - u_1) - u_1 u_2 \ - \ \lambda(1 - e^{-5u_1}) \, , \\[2em]
u_2' &= \quad -u_2 \ + \ 3u_1 u_2 \, .
\end{cases}
$$

Here u_1 may be thought of as "fish" and u_2 as "sharks", while the term

$$
\lambda \left(1 - e^{-5u_1}\right) \, ,
$$

represents "fishing", with "fishing-quota" λ .

When $\lambda = 0$ the *stationary solutions* are

$$
\left. \begin{array}{rcl}
3u_1(1 - u_1) - u_1 u_2 &=& 0 \\[1em]
-u_2 \ + \ 3u_1 u_2 &=& 0
\end{array} \right\} \ \Rightarrow \ (u_1, u_2) \ = \ (0,0) \, , \ (1,0) \, , \ (\tfrac{1}{3}, 2) \, .
$$

4

The Jacobian matrix is

$$J = \begin{pmatrix} 3 - 6u_1 - u_2 - 5\lambda e^{-5u_1} & -u_1 \\ 3u_2 & -1 + 3u_1 \end{pmatrix} = J(u_1, u_2; \lambda) .$$

$$J(0, 0; 0) = \begin{pmatrix} 3 & 0 \\ 0 & -1 \end{pmatrix}; \quad \text{eigenvalues 3, -1 \quad (unstable)} .$$

$$J(1, 0; 0) = \begin{pmatrix} -3 & -1 \\ 0 & 2 \end{pmatrix}; \quad \text{eigenvalues -3, 2 \quad (unstable)} .$$

$$J(\frac{1}{3}, 2; 0) = \begin{pmatrix} -1 & -\frac{1}{3} \\ 6 & 0 \end{pmatrix}; \quad \text{eigenvalues } -\frac{1}{2} \pm i \sqrt{\frac{7}{2}} \quad \text{(stable)} .$$

All three Jacobians at $\lambda = 0$ are nonsingular.

Thus, by the IFT, all three stationary points persist for (small) $\lambda \neq 0$.

In this problem we can *explicitly* find all solutions (see Figure 1) :

I :

$$(u_1, u_2) = (0, 0) .$$

II :

$$u_2 = 0 , \qquad \lambda = \frac{3u_1(1 - u_1)}{1 - e^{-5u_1}} .$$

$$\left(\text{Note that} \lim_{u_1 \to 0} \lambda = \frac{3}{5} . \right)$$

III :

$$u_1 = \frac{1}{3}, \qquad u_2 = 2 - 3\lambda(1 - e^{-5/3}) .$$

These solution families intersect at two *branch points*, one of which is
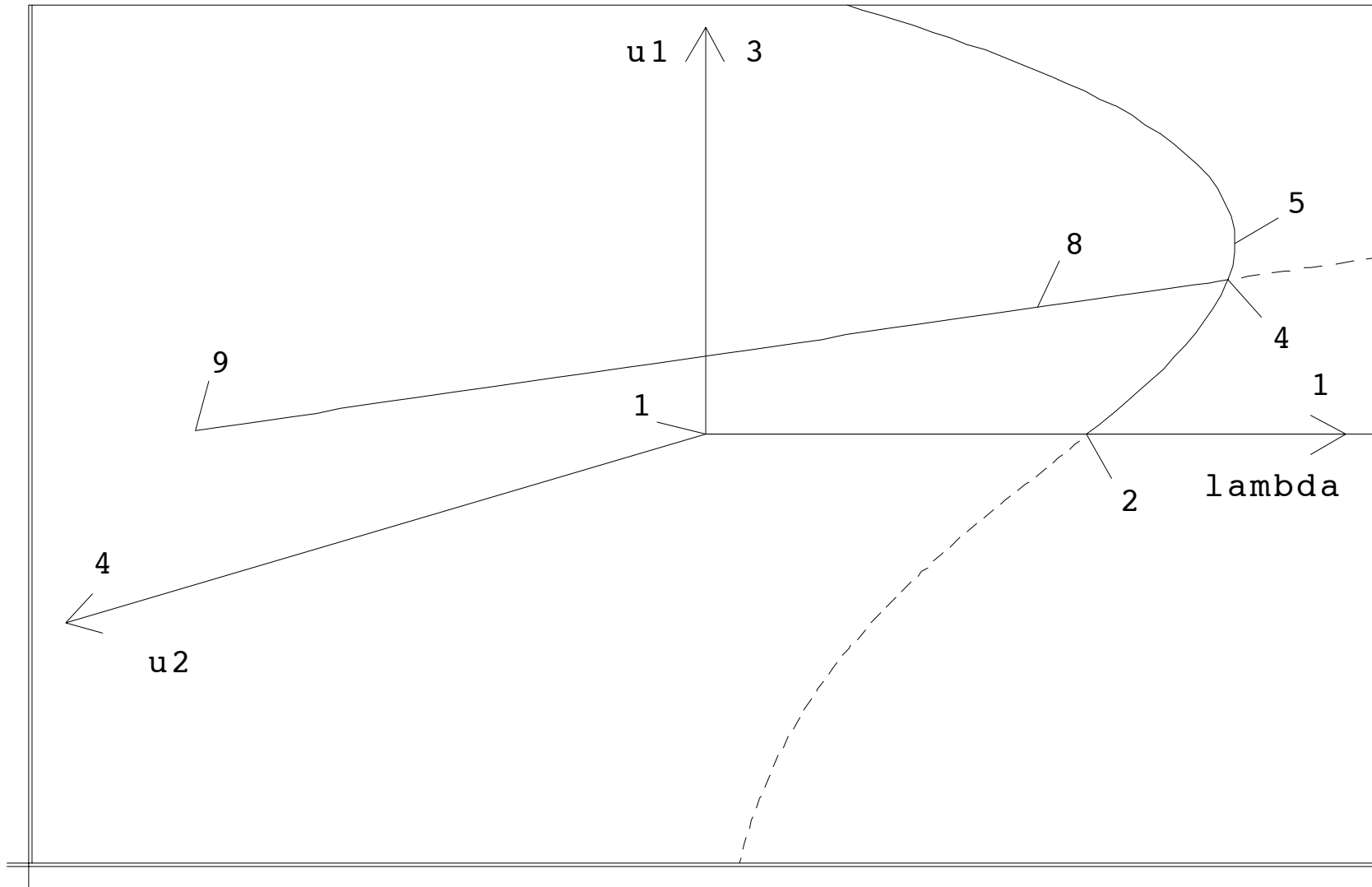
$$(u_1, u_2, \lambda) = (0, 0, 3/5) .$$

Figure 1: Stationary solution branches of the predator-prey model. Solutions 2 and 4 are branch points. Solution 8 is a Hopf bifurcation point.
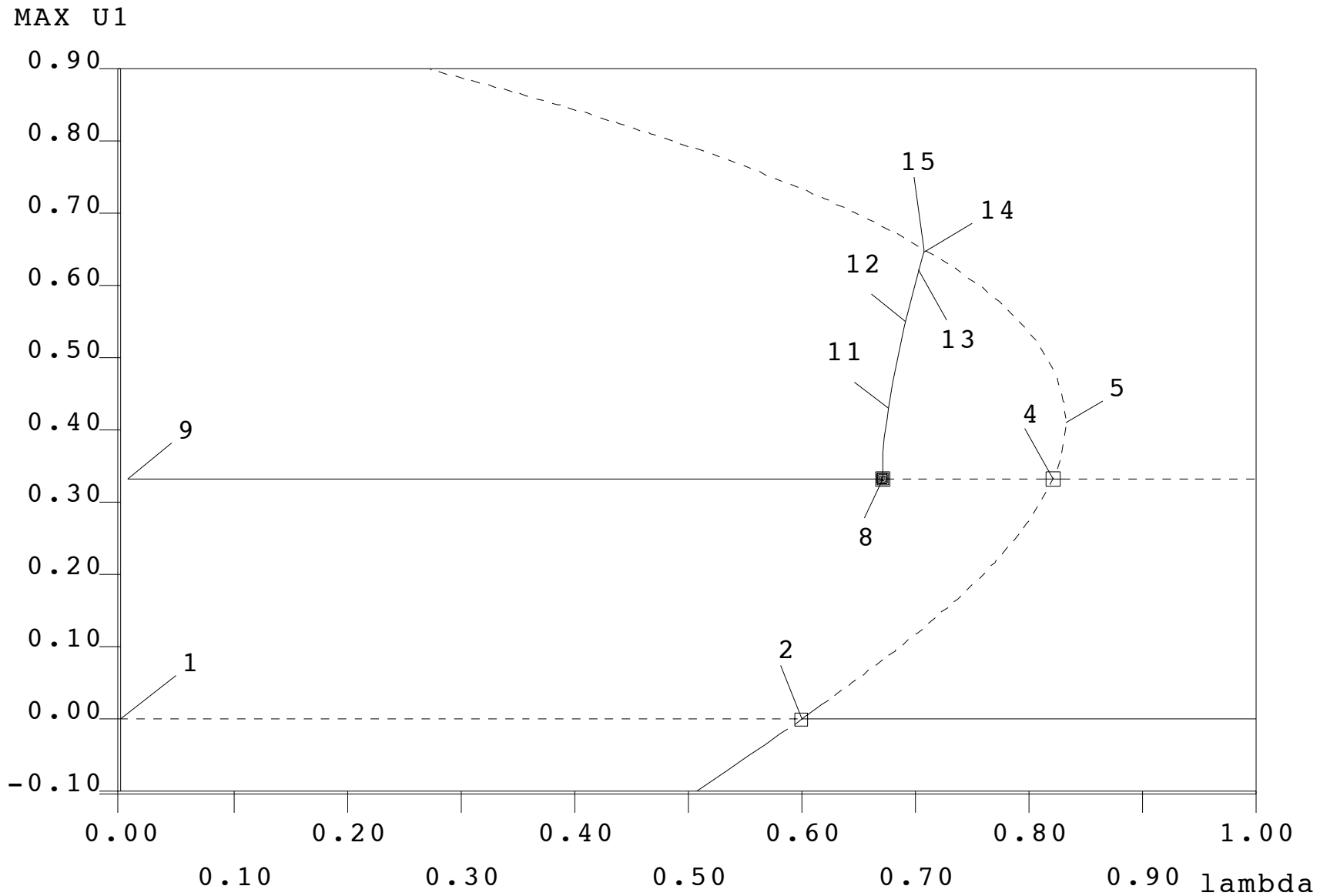
Figure 2: Bifurcation diagram of the predator-prey model. The periodic solution branch is also shown. Solid/dashed lines denote stable/unstable solution. Open squares are branch points; the solid square is a Hopf bifurcation.
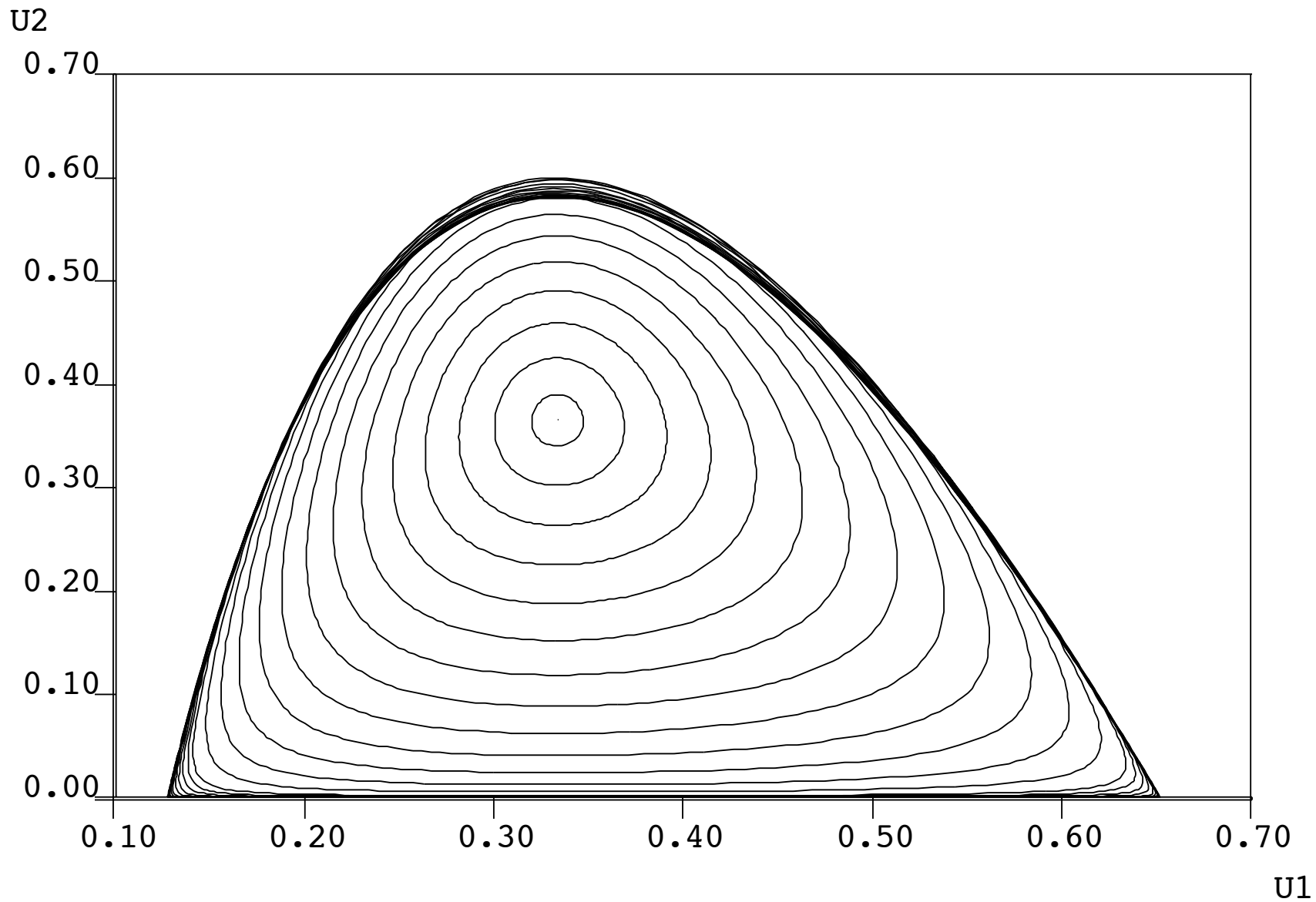
Figure 3: Some periodic solutions of the predator-prey model. The final orbits are very close to a heteroclinic cycle.

- Stability of branch I :

$$J((0,0);\lambda) \;=\; \begin{pmatrix} 3-5\lambda & 0 \\ 0 & -1 \end{pmatrix}; \quad \text{eigenvalues } 3-5\lambda, \; -1 \; .$$

Hence the trivial solution is :

$$\text{unstable if } \lambda < 3/5 \; ,$$

and

$$\text{stable if } \lambda > 3/5 \; ,$$

as indicated in Figure 2.

- Stability of branch II :

This branch has no stable positive solutions.

- Stability of branch III :

At
$$\lambda_H \approx 0.67 ,$$
(Solution 8 in Figure 2) the complex eigenvalues cross the imaginary axis.

This crossing is a *Hopf bifurcation.*

Beyond λ_H there are *periodic solutions* of increasing period T .
(See Figure 3 for some representative periodic orbits.)

The period becomes infinite at $\lambda = \lambda_\infty \approx 0.7$.

This final orbit is called a *heteroclinic cycle.*

From Figure 2 we can deduce the solution behavior for (slowly) increasing λ :

- Branch III is followed until λ_H .

- Periodic solutions of increasing period until $\lambda = \lambda_\infty$.

- Collapse to trivial solution (Branch I).

DEMO.

Use AUTO to repeat the numerical calculations (demo `pp2`) .

Sketch phase plane diagrams for $\lambda = 0,\ 0.5,\ 0.68,\ 0.70,\ 0.71$.

The Gelfand-Bratu Problem

$$\begin{cases} u''(x) \ - \ \lambda \ e^{u(x)} \quad = \quad 0 \ , \quad \forall x \in [0,1] \ , \\[2ex] u(0) \ = \ u(1) \quad\quad = \quad 0 \ . \end{cases}$$

If $\lambda = 0$ then $u(x) \equiv 0$ is a solution.

This solution is isolated, so that there is a continuation

$$u \ = \ \tilde{u}(\lambda) \ , \quad \text{for} \ \ |\lambda| \ \ \text{small} \ .$$

DEMO. Compute the solution branch of the Gelfand-Bratu problem as represented in Figures 4 and 5. (AUTO demo `exp`.)
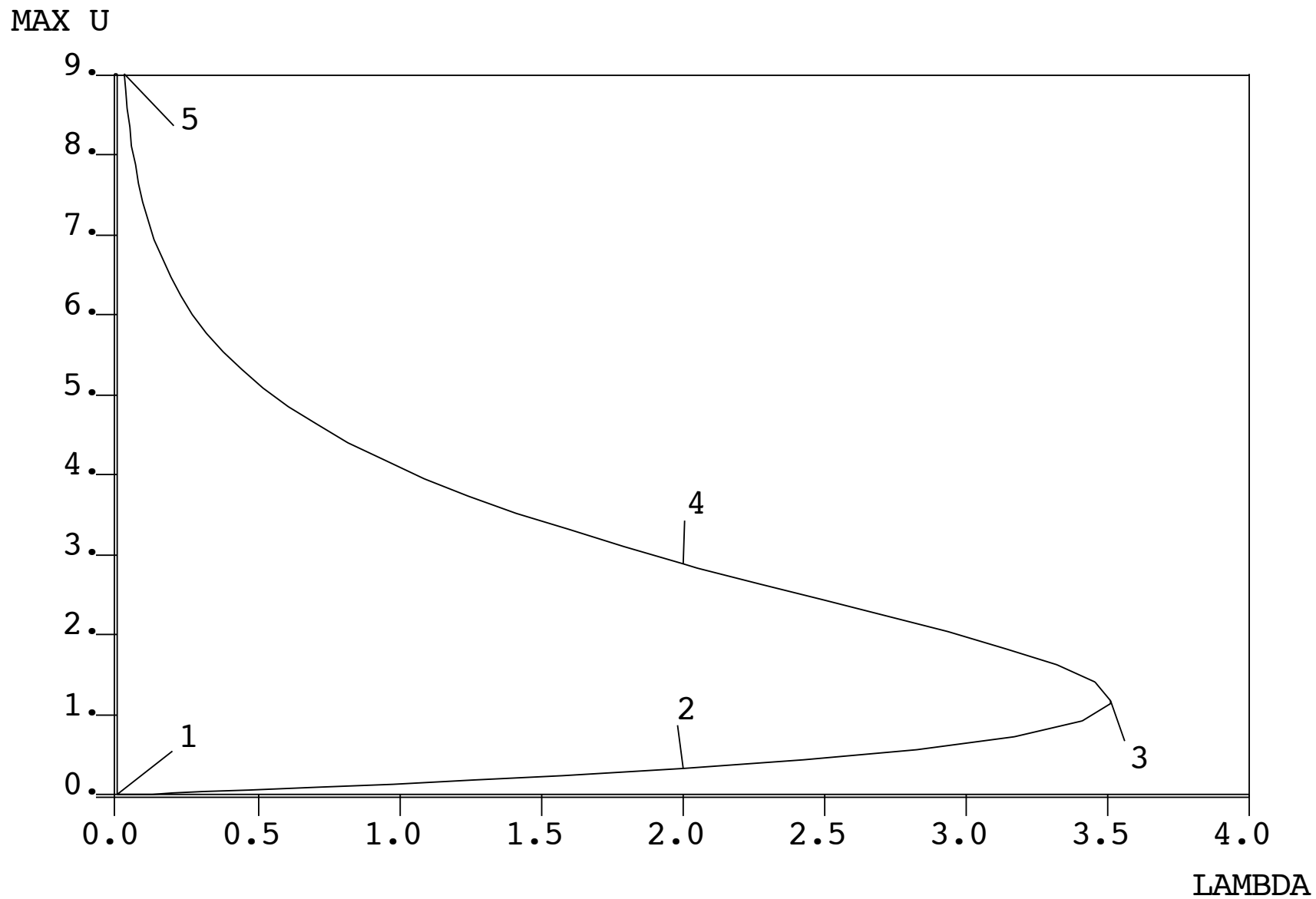
13

Figure 4: Bifurcation diagram of the Gelfand-Bratu equation. There are two solutions for $0 < \lambda < \lambda_C$, where $\lambda_C \approx 3.51$.
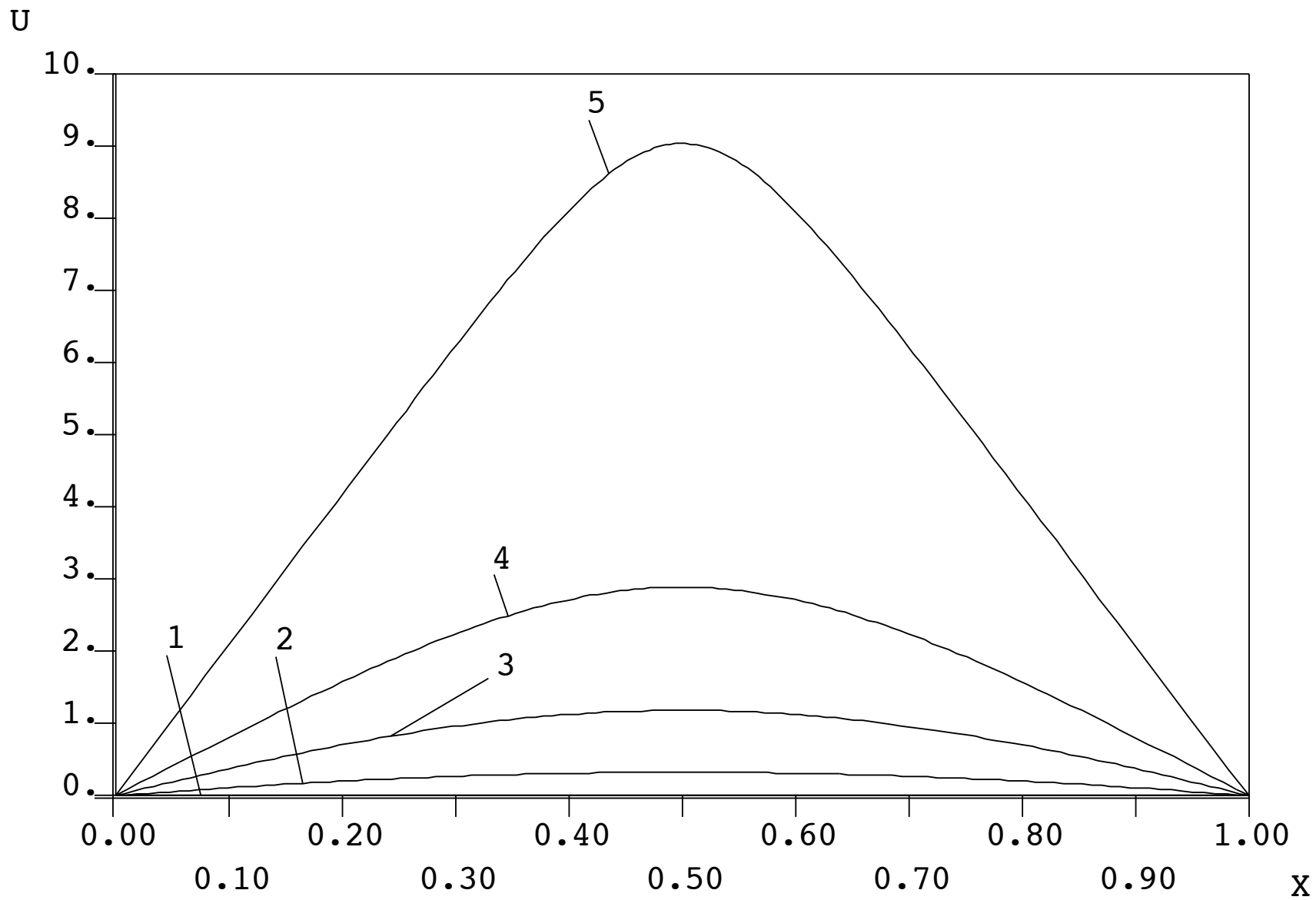
Figure 5: Some solutions to the Gelfand-Bratu equation.

Continuation of Solutions

We discuss the computation of families of solutions to nonlinear equations.

Consider the equation

$$G(u, \lambda) = 0 , \qquad u , \; G(\cdot, \cdot) \in \mathrm{R}^n , \quad \lambda \in \mathrm{R} .$$

Let

$$x \equiv (u , \; \lambda) .$$

Then the equation can be written

$$G(x) = 0 , \qquad G : \mathrm{R}^{n+1} \rightarrow \mathrm{R}^n .$$

DEFINITION.

A solution x_0 of $G(x) = 0$ is *regular* if the n by $n+1$ matrix

$$G_x^0 \equiv G_x(x_0) ,$$

has maximal rank, *i.e.*, if

$$\mathrm{Rank}(G_x^0) = n .$$

In the parameter formulation,

$$G(u, \lambda) = 0,$$

we have

$$\text{Rank}(G_x^0) = \text{Rank}(G_u^0 \mid G_\lambda^0) = n \iff \begin{cases} \text{(i)} \ G_u^0 \text{ is nonsingular,} \\ \\ \quad \text{or} \\ \\ \text{(ii)} \begin{cases} dim \ \mathcal{N}(G_u^0) = 1, \\ \text{and} \\ G_\lambda^0 \notin \mathcal{R}(G_u^0). \end{cases} \end{cases}$$

Above,

$$\mathcal{N}(G_u^0) \ \text{denotes the } null \ space \text{ of } \ G_u^0,$$

and

$$\mathcal{R}(G_u^0) \text{ denotes the } range \text{ of } \ G_u^0,$$

i.e., the linear space spanned by the n columns of G_u^0.

FACT: Let
$$x_0 \;\equiv\; (\; u_0\;,\; \lambda_0\;)$$
be a regular solution of
$$G(x) \;=\; 0 \;.$$
Then, near x_0 , there exists a unique one-dimensional continuum of solutions

$$x(s) \qquad \text{with} \quad x(0) \;=\; x_0 \;.$$

PROOF. Since

$$\text{Rank}(\; G_x^0\;) \;=\; \text{Rank}(\; G_u^0 \mid G_\lambda^0\;) \;=\; n \;,$$

then either G_u^0 is nonsingular and by the IFT we have

$$u \;=\; u(\lambda) \quad \text{near} \quad x_0 \;,$$

or else we can interchange colums in the Jacobian G_x^0 to see that the solution can locally be parametrized by one of the components of u .

Thus a unique solution family passes through a regular solution. ●

REMARKS.

Such a continuum of solutions is called a *solution family* or a *solution branch.*

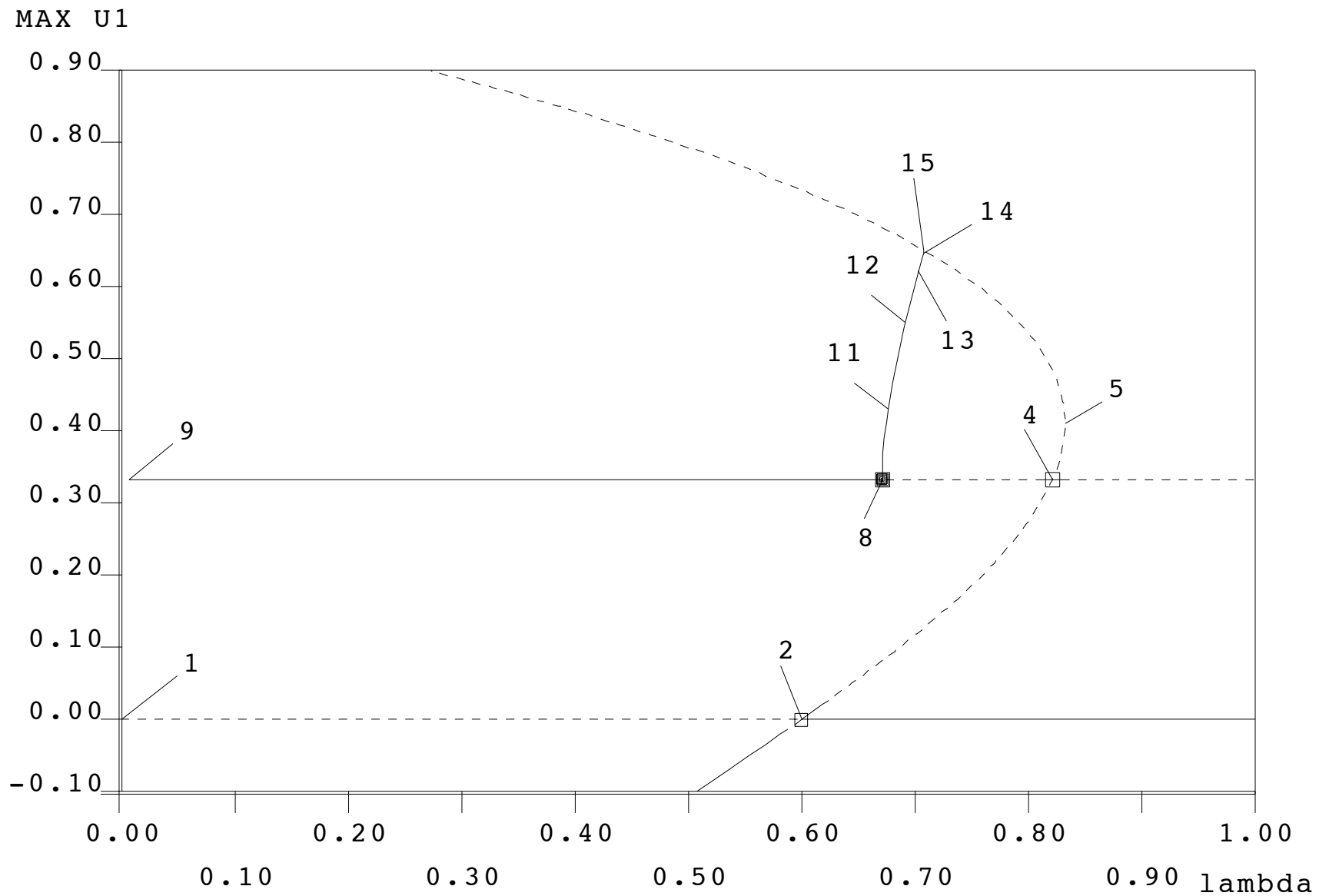Case (ii) above is that of a *simple fold* (or *saddle-node bifurcation*).

Figure 6: Note the fold at Solution 5 in the predator-prey model.

Keller's Pseudo-Arclength Continuation

This method allows continuation of a branch past folds.

Suppose we have a solution (u_0, λ_0) of

$$G(\ u\ ,\ \lambda\ )\ =\ 0\ ,$$

as well as the direction vector of the solution branch $(\dot{u}_0, \dot{\lambda}_0)$.

Pseudo-arclength continuation solves the following equations for (u_1, λ_1) :

$$G(u_1, \lambda_1)\ =\ 0\ ,$$

$$(u_1\ -\ u_0)^*\ \dot{u}_0\ +\ (\lambda_1\ -\ \lambda_0)\ \dot{\lambda}_0\ -\ \Delta s\ =\ 0\ .$$

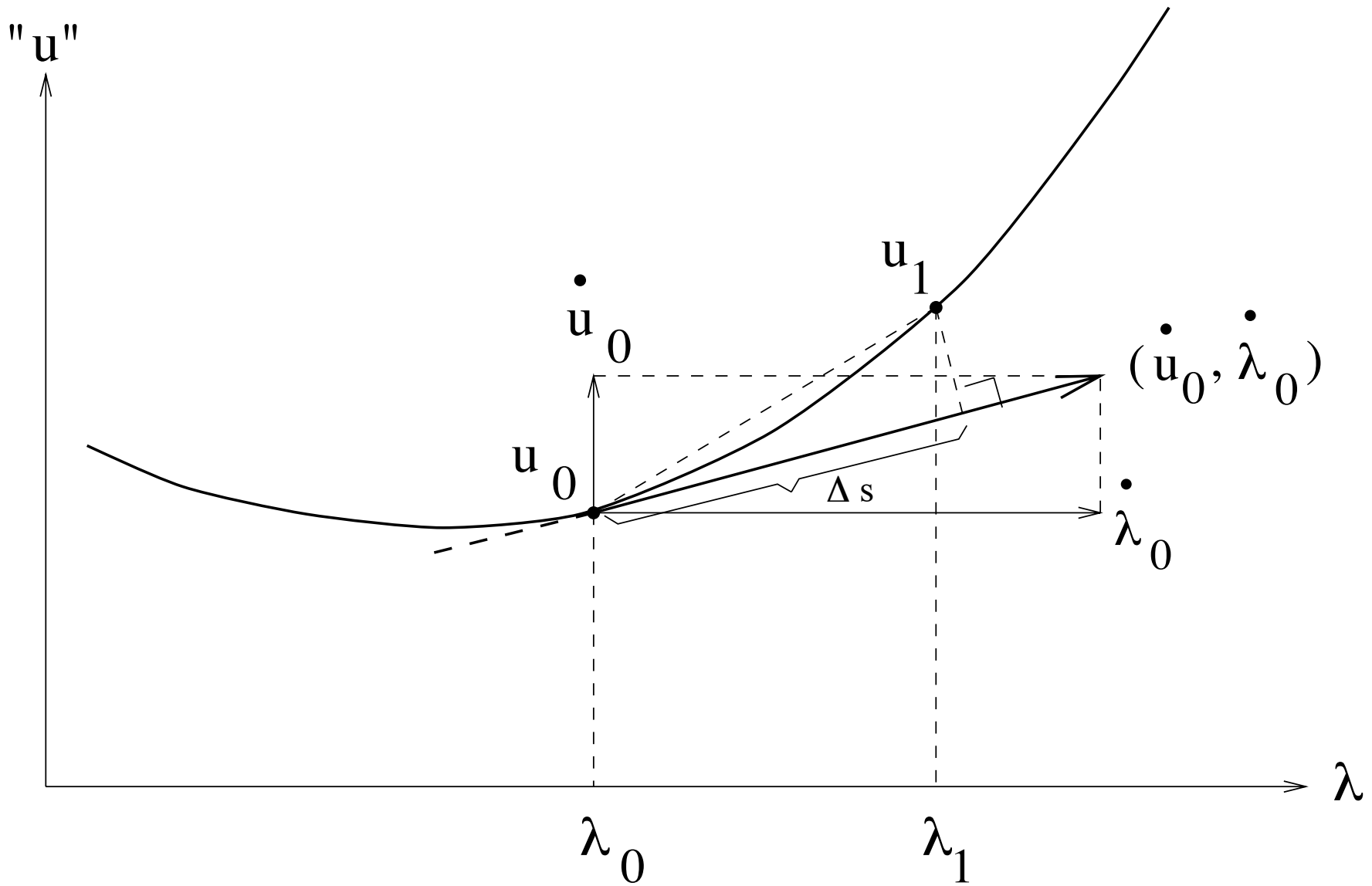See Figure 7 for a graphical interpretation.

Figure 7: Graphical interpretation of pseudo-arclength continuation.

Newton's method for pseudo-arclength continuation :

$$
\begin{pmatrix} (G_u^1)^{(\nu)} & (G_\lambda^1)^{(\nu)} \\ \dot{u}_0^* & \dot{\lambda}_0 \end{pmatrix} \begin{pmatrix} \Delta u_1^{(\nu)} \\ \Delta \lambda_1^{(\nu)} \end{pmatrix} = - \begin{pmatrix} G(u_1^{(\nu)}, \lambda_1^{(\nu)}) \\ (u_1^{(\nu)} - u_0)^* \dot{u}_0 - (\lambda_1^{(\nu)} - \lambda_0)\dot{\lambda}_0 - \Delta s \end{pmatrix} .
$$

Next direction vector :

$$
\begin{pmatrix} G_u^1 & G_\lambda^1 \\ \dot{u}_0^* & \dot{\lambda}_0 \end{pmatrix} \begin{pmatrix} \dot{u}_1 \\ \dot{\lambda}_1 \end{pmatrix} = \begin{pmatrix} 0 \\ 1 \end{pmatrix} .
$$

REMARKS .

- In practice $(\dot{u}_1, \dot{\lambda}_1)$ can be computed with one extra backsubstitution.

- The orientation of the branch is preserved if Δs is sufficiently small.

- The direction vector must be rescaled, so that indeed $\parallel \dot{u}_1 \parallel^2 + \dot{\lambda}_1^2 = 1$.

Parameter-independent representation

Let

$$x \equiv (u, \lambda) \in \mathrm{R}^{n+1} \ .$$

Then pseudo-arclength continuation can be written as

$$G(x_1) = 0 \ ,$$

$$(x_1 - x_0)^* \dot{x}_0 - \Delta s = 0 \ , \qquad (\| \dot{x}_0 \| = 1) \ .$$
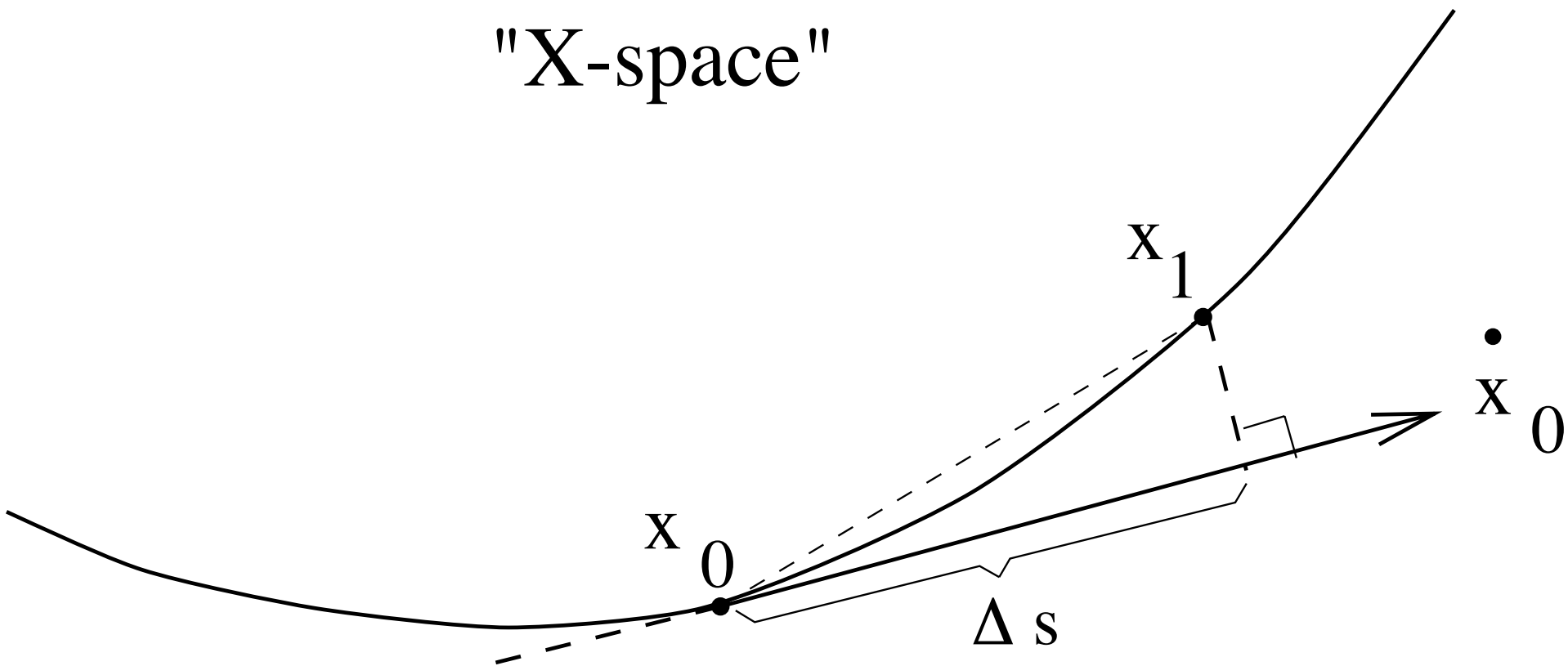
(See Figure 8 for a graphical interpretation.)

Figure 8: Parameter-independent pseudo-arclength continuation.

FACT:

The pseudo-arclength Jacobian is nonsingular at a regular solution point.

PROOF. The matrix in Newton's method at $\Delta s = 0$ is

$$\begin{pmatrix} G_x^0 \\ \dot{x}_0^* \end{pmatrix} .$$

At a regular solution we have

$$\mathcal{N}(G_x^0) = \text{Span}\{\dot{x}_0\} .$$

It is now easy to see that

$$\begin{pmatrix} G_x^0 \\ \dot{x}_0^* \end{pmatrix}$$

is nonsingular at a regular solution.

EXAMPLE. The Gelfand-Bratu problem :

$$u''(x) \; + \; \lambda \, e^{u(x)} \; = \; 0 \quad \text{for} \quad x \in [0,1] \,, \qquad u(0) \; = \; 0 \,, \qquad u(1) \; = \; 0 \,.$$

Fact: If $\lambda = 0$ then $u(x) \equiv 0$ is an isolated solution.

Discretize by introducing a mesh ,

$$0 \; = \; x_0 \; < \; x_1 \; < \; \cdots \; < \; x_N \; = \; 1 \,,$$

$$x_j \; - \; x_{j-1} \; = \; h \,, \quad (1 \le j \le N) \,, \qquad h \; = \; 1/N \,.$$

The discrete equations are :

$$\frac{u^{j+1} \; - \; 2u^j \; + \; u^{j-1}}{h^2} \; + \; \lambda \, e^{u^j} \; = \; 0 \,, \qquad j = 1, \cdots, N-1 \,,$$

with $u^0 \; = \; u^N \; = \; 0$.

Let

$$U \equiv (u^1, u^2, \cdots, u^{N-1}).$$

Then we can write the above as

$$G(U, \lambda) = 0,$$

where

$$G : \mathrm{R}^{N-1} \times \mathrm{R} \to \mathrm{R}^{N-1}.$$

Pseudo-arclength continuation:

$$G(\ U_1\ ,\ \lambda_1\ )\ =\ 0\ ,$$

$$(U_1\ -\ U_0\ )^*\ \dot{U}_0\ +\ (\lambda_1\ -\ \lambda_0)\ \dot{\lambda}_0\ -\ \Delta s\ =\ 0\ .$$

Repeat the above procedure to find $U_2\ ,\ U_3\ ,\ \cdots$.

The matrix in Newton's method is bordered tridiagonal :

Such linear systems can be solved very efficiently.

DEMO.

Compute the branch of complex solutions that bifurcates from the fold in the complexified Gelfand-Bratu problem. (AUTO demo `ezp`.)
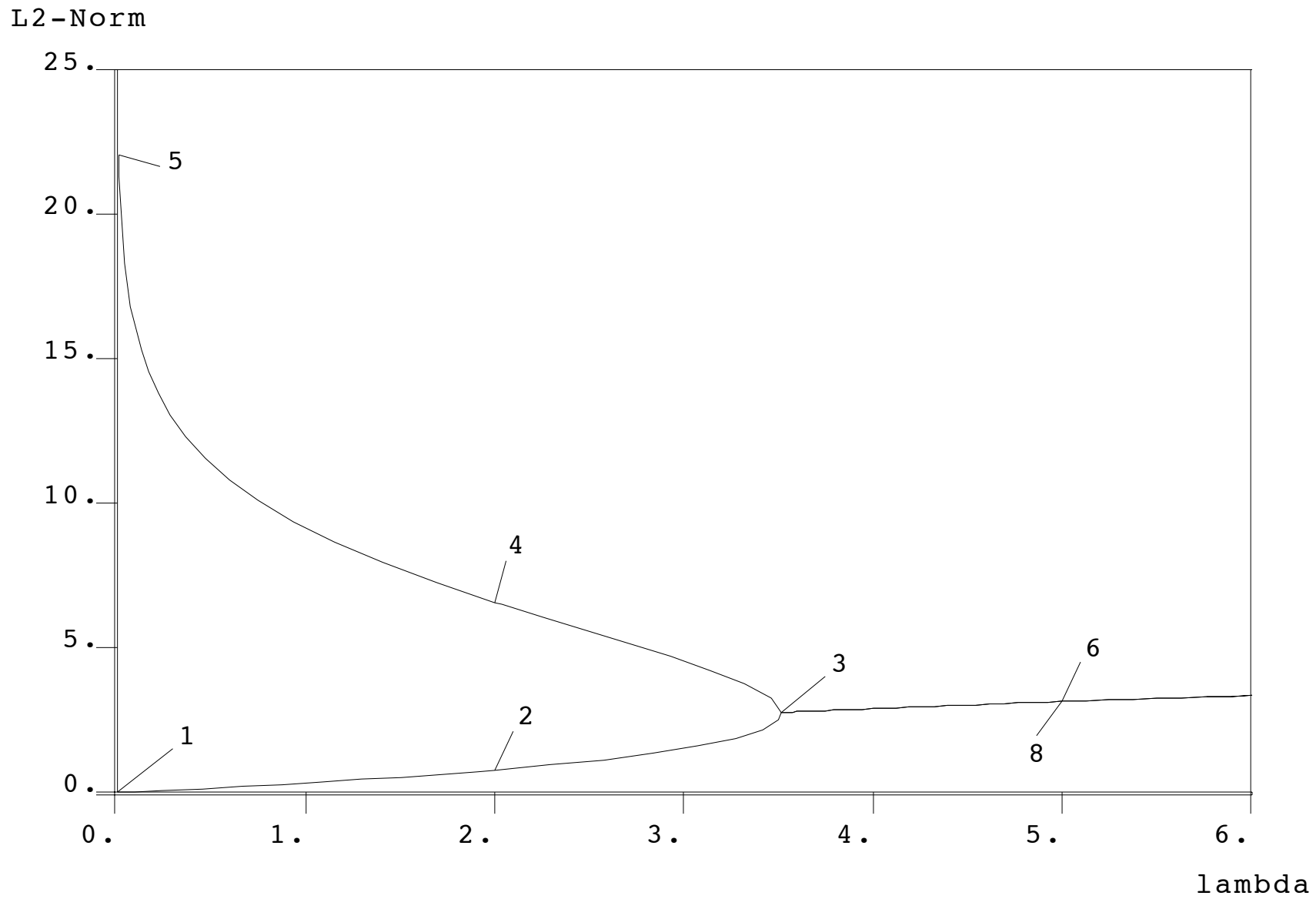
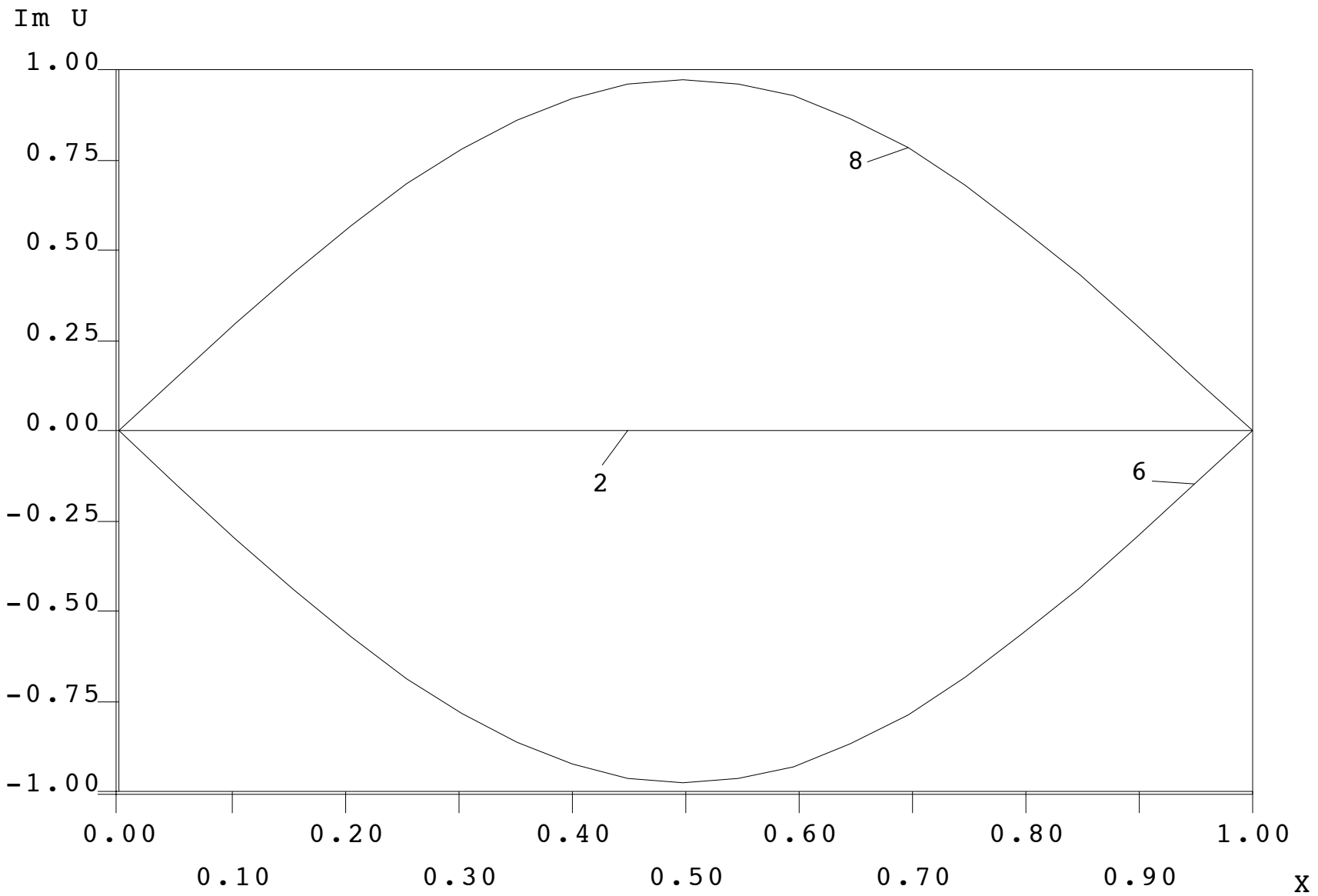Figure 9: The bifurcation diagram of the complex Gelfand-Bratu equation.

Figure 10: Imaginary part of solutions to the complex Gelfand-Bratu equation.

Boundary Value Problems

Boundary Value Problems.

Consider the first order system of ordinary differential equations

$$u'(t) \ - \ f(\ u(t) \ , \ \mu \ , \ \lambda \ ) \ = \ 0 \ , \qquad t \in [0, 1] \ ,$$

where

$$u(\cdot) \ , \ f(\cdot) \in \mathrm{R}^n \ , \qquad \lambda \in \mathrm{R}, \qquad \mu \in \mathrm{R}^{n_\mu} \ ,$$

subject to boundary conditions

$$b(\ u(0) \ , \ u(1) \ , \ \mu \ , \ \lambda \ ) \ = \ 0 \ , \qquad b(\cdot) \in \mathrm{R}^{n_b} \ ,$$

and integral constraints

$$\int_0^1 \ q(\ u(s) \ , \ \mu \ , \ \lambda \ ) \ ds \ = \ 0 \ , \qquad q(\cdot) \in \mathrm{R}^{n_q} \ .$$

REMARKS .

- We must solve the boundary value problem (BVP) for $u(\cdot)$ and μ .

- Think of λ as the parameter in which a solution (u, μ) is continued.

- In order for problem to be formally well posed we require that

$$n_\mu \;=\; n_b \;+\; n_q \;-\; n \;\geq\; 0 \, .$$

- A simple case is

$$n_q \;=\; 0 \, , \qquad n_b \;=\; n \, , \qquad \text{for which} \quad n_\mu \;=\; 0 \, .$$

Discretization

Here we discuss the method of "orthogonal collocation with piecewise polynomials", for solving boundary value problems. This method is very accurate, and allows adaptive mesh-selection.

Orthogonal Collocation

The equations are

$$u'(t) \; - \; f(\, u(t) \, , \; \mu \, , \; \lambda \,) \; = \; 0 \, , \qquad t \in [0, 1] \, ,$$

where
$$u(\cdot) \, , \; f(\cdot) \in \mathrm{R}^n \, , \qquad \lambda \in \mathrm{R} \, , \qquad \mu \in \mathrm{R}^{n_\mu} \, ,$$

subject to boundary conditions

$$b(\, u(0) \, , \; u(1) \, , \; \mu \, , \; \lambda \,) \; = \; 0 \, , \qquad b(\cdot) \in \mathrm{R}^{n_b} \, ,$$

and integral constraints

$$\int_0^1 q(\, u(s) \, , \; \mu \, , \; \lambda \,) \, ds \; = \; 0 \, , \qquad q(\cdot) \in \mathrm{R}^{n_q} \, ,$$

with
$$n_\mu \; = \; n_b \; + \; n_q \; - \; n \; \geq \; 0 \, .$$

The "extra" parameter λ will be freed in continuation.

Introduce a mesh

$$\{ \; 0 \; = \; t_0 \; < \; t_1 \; < \; \cdots \; < \; t_N \; = \; 1 \; \} \, ,$$

where

$$\Delta t_j \; \equiv \; t_j \; - \; t_{j-1} \, , \qquad (1 \le j \le N) \, ,$$

Define the space of *piecewise polynomials* $\mathcal{P}_h^m$ as

$$\mathcal{P}_h^m \; = \; \{ \; p_h \in C[0,1] \; : \; p_h \big|_{[t_{j-1}, t_j]} \in \mathcal{P}^m \; \} \, ,$$

where $\mathcal{P}^m$ is the space of polynomials of degree less than or equal to m .

The collocation method consists of finding

$$p_h \in \mathcal{P}_h^m , \qquad \mu \in \mathrm{R}^{n_\mu} ,$$

such that the following *collocation equations* are satisfied:

$$p_h'(z_{j,i}) = f(p_h(z_{j,i}) , \mu, \lambda) , \qquad j = 1, \cdots, N , \quad i = 1, \cdots, m ,$$

and such that p_h satisfies the boundary and integral conditions.

The *collocation points* $z_{j,i}$ in each subinterval

$$[t_{j-1} , t_j] ,$$

are the (scaled) roots of the mth-degree orthogonal polynomial (*Gauss points*) .

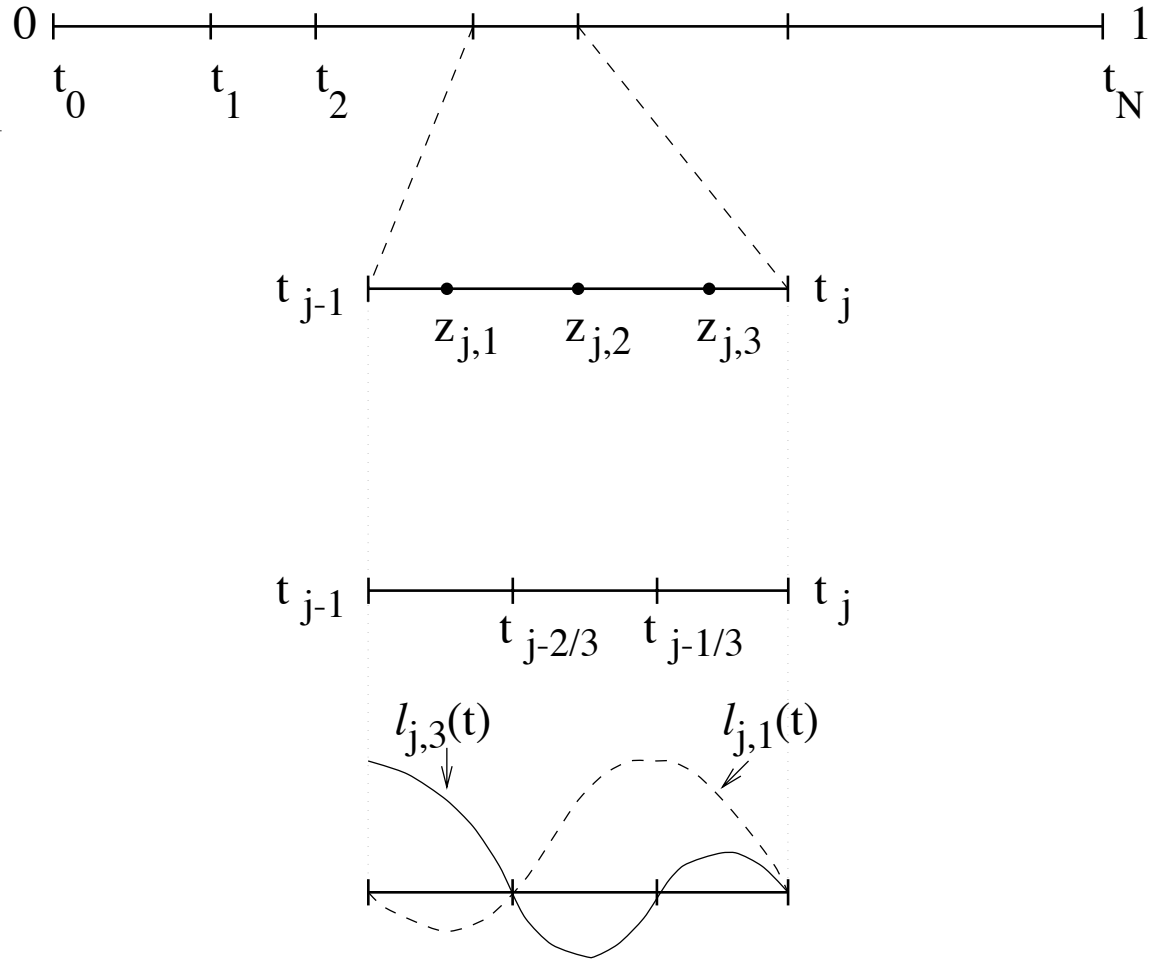See Figure 11 for a graphical interpretation.

Figure 11: The mesh $\{0 = t_0 < t_1 < \cdots < t_N = 1\}$. Collocation points and "extended-mesh points" are shown for the case $m = 3$, in the jth mesh interval. Also shown are two of the four local Lagrange basis polynomials.

41

Since each local polynomial is determined by

$$(m + 1)\, n\ ,$$

coefficients, the total number of degrees of freedom (considering λ as fixed) is

$$(m + 1)\, n\, N\ +\ n_\mu\ .$$

This is matched by the total number of equations :

$$\text{collocation}:\quad m\, n\, N\ ,$$

$$\text{continuity}:\quad (N - 1)\, n\ ,$$

$$\text{constraints}:\quad n_b\ +\ n_q\quad (=\ n\ +\ n_\mu)\ .$$

Assume that the solution $u(t)$ is sufficiently smooth.

Then the global accuracy of the *orthogonal collocation method* with piecewise polynomials, is of order m, *i.e.*,

$$\| p_h - u \|_\infty = \mathcal{O}(h^m) .$$

At the main meshpoints t_j we have *superconvergence* :

$$max_j \mid p_h(t_j) - u(t_j) \mid = \mathcal{O}(h^{2m}) .$$

The scalar variables μ are also superconvergent.

Implementation

For each subinterval $[\,t_{j-1}\,,\,t_j\,]$, introduce the Lagrange basis polynomials

$$\{\,\ell_{j,i}(t)\,\}\,,\qquad j=1,\cdots,N\,,\quad i=0,1,\cdots,m\,,$$

defined by

$$\ell_{j,i}(t)\;=\;\prod_{k=0,k\neq i}^{m}\;\frac{t-t_{j-\frac{k}{m}}}{t_{j-\frac{i}{m}}\;-\;t_{j-\frac{k}{m}}}\;,$$

where

$$t_{j-\frac{i}{m}}\;\equiv\;t_j\;-\;\frac{i}{m}\,\Delta t_j\;.$$

The local polynomials can then be written

$$p_j(t)\;=\;\sum_{i=0}^{m}\ell_{j,i}(t)\,u_{j-\frac{i}{m}}\;.$$

With the above choice of basis

$$u_j\;\sim\;u(t_j)\qquad\text{and}\qquad u_{j-\frac{i}{m}}\;\sim\;u\big(t_{j-\frac{i}{m}}\big)\,,$$

where $u(t)$ is the solution of the continuous problem.

The collocation equations are

$$p'_j(z_{j,i}) = f(p_j(z_{j,i}) , \mu , \lambda) , \qquad i = 1, \cdots, m, \quad j = 1, \cdots, N .$$

The discrete boundary conditions are

$$b_i(u_0 , u_N , \mu , \lambda) = 0 , \qquad i = 1, \cdots, n_b .$$

The integrals can be discretized as

$$\sum_{j=1}^{N} \sum_{i=0}^{m} \omega_{j,i} \, q_k (u_{j-\frac{i}{m}} , \mu , \lambda) = 0 , \qquad k = 1, \cdots, n_q ,$$

where the $\omega_{j,i}$ are the Lagrange quadrature coefficients.

The pseudo-arclength equation is

$$\int_0^1 (u(t) - u_0(t))^* \dot{u}_0(t) \, dt + (\mu - \mu_0)^* \dot{\mu}_0 + (\lambda - \lambda_0) \dot{\lambda}_0 - \Delta s = 0 \,,$$

where

$$(\, u_0 \,, \, \mu_0 \,, \, \lambda_0 \,) \,,$$

is the previously computed point on the solution branch, and

$$(\, \dot{u}_0 \,, \, \dot{\mu}_0 \,, \, \dot{\lambda}_0 \,) \,,$$

is the normalized direction of the branch at that point.

The discretized pseudo-arclength equation is

$$\sum_{j=1}^N \sum_{i=0}^m \omega_{j,i} \, [\, u_{j-\frac{i}{m}} - (u_0)_{j-\frac{i}{m}} \,]^* \, (\dot{u}_0)_{j-\frac{i}{m}}$$

$$+ \, (\mu - \mu_0)^* \dot{\mu}_0 + (\lambda - \lambda_0) \dot{\lambda}_0 - \Delta s = 0 \,.$$

Numerical Linear Algebra

The complete discretization consists of

$$m \, n \, N \;\; + \;\; n_b \;\; + \;\; n_q \;\; + \;\; 1 \, ,$$

nonlinear equations, in the unknowns

$$\{u_{j-\frac{i}{m}}\} \in \mathrm{R}^{mnN+n} \, , \qquad \mu \in \mathrm{R}^{n_\mu} \, , \qquad \lambda \in \mathrm{R} \, .$$

- These equations can be solved by a Newton-Chord iteration.

- The structure of the linearized systems is illustrated in Figure 12.

- A solution method of the linear systems is illustrated in Figures 13-16.

- The indicated operations are also carried out on the right hand side.

- The right hand side is not shown in the Figures.
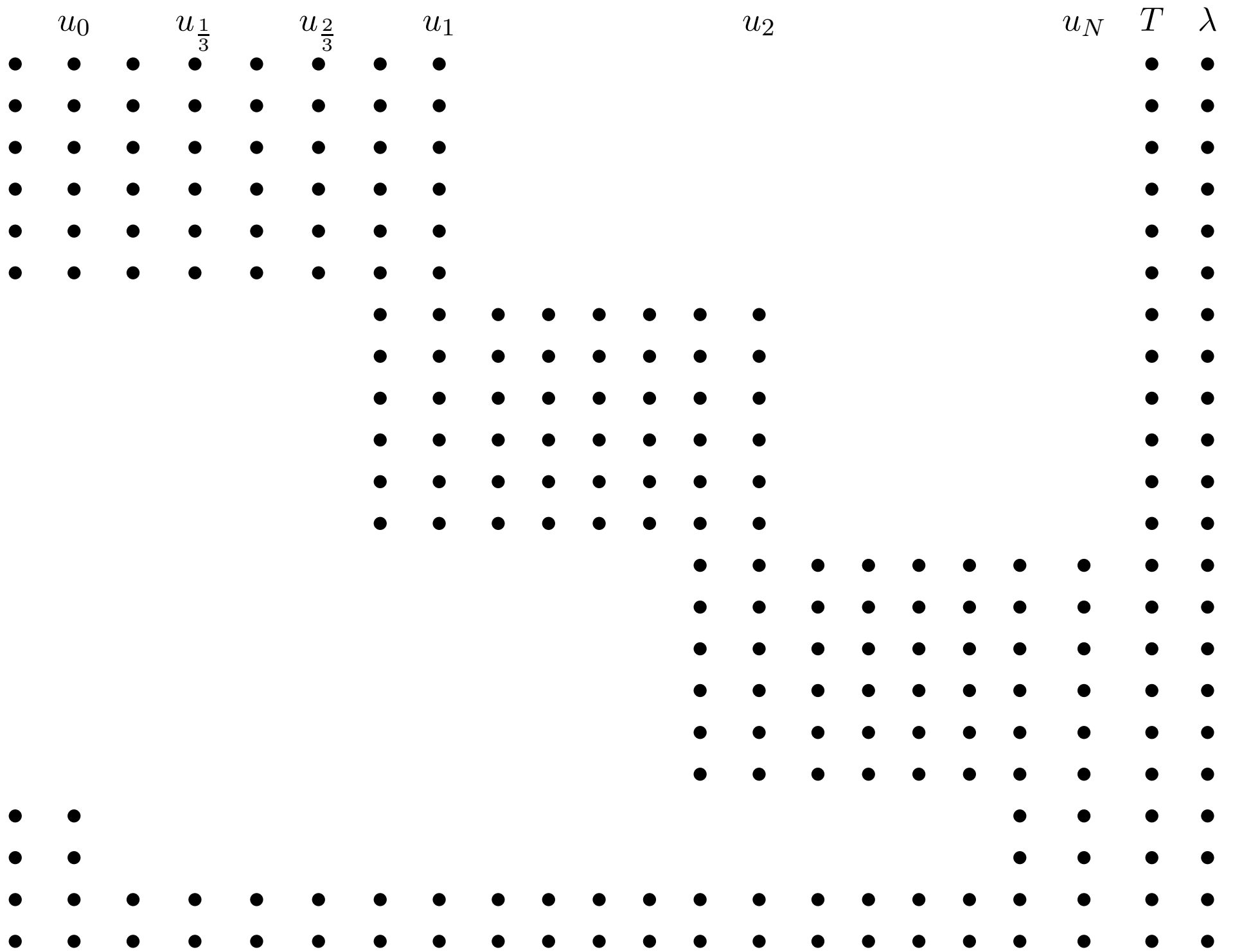
Figure 12:

CAPTION FOR FIGURE 12 :

- Structure of the Jacobian for the case of $n = 2$ differential equations.

- Number of mesh intervals : $N = 3$.

- Number of collocation points per mesh interval : $m = 3$.

- Number of boundary conditions : $n_b = 2$.

- Number of integral constraints : $n_q = 1$.

- The last row corresponds to the pseudo-arclength equation, which is not included in the $n_q = 1$ count.

- In a typical problem N will be larger, say, $N = 5$, for "very easy" problems, and $N = 200$, for "very difficult" problems.

- The "standard" choice of the number of collocation points per mesh interval is $m = 4$.
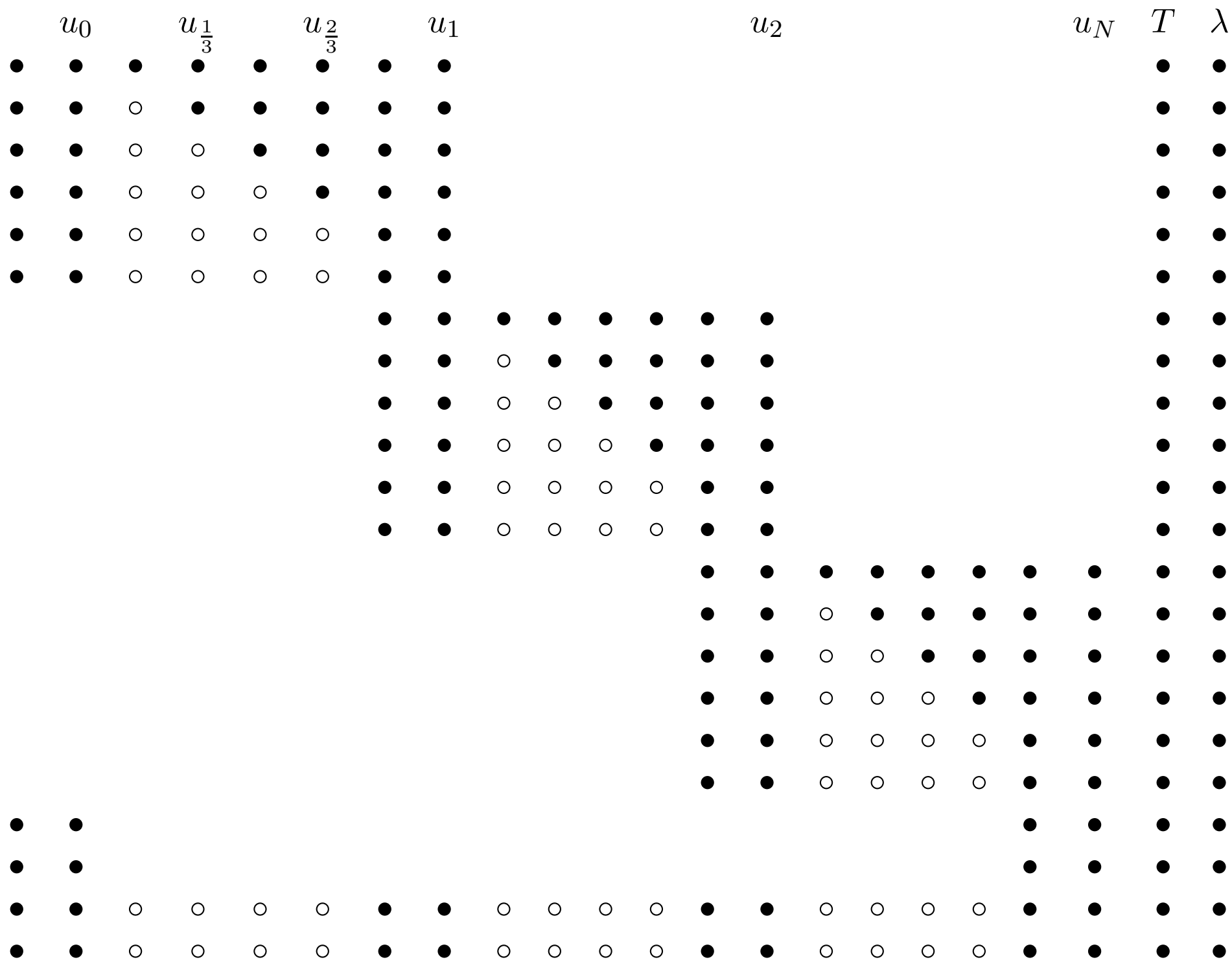
Figure 13:

CAPTION FOR FIGURE 13 :

- The system after "*condensation of parameters*".

- The entries marked " ∘ " have been eliminated by Gauss elimination.

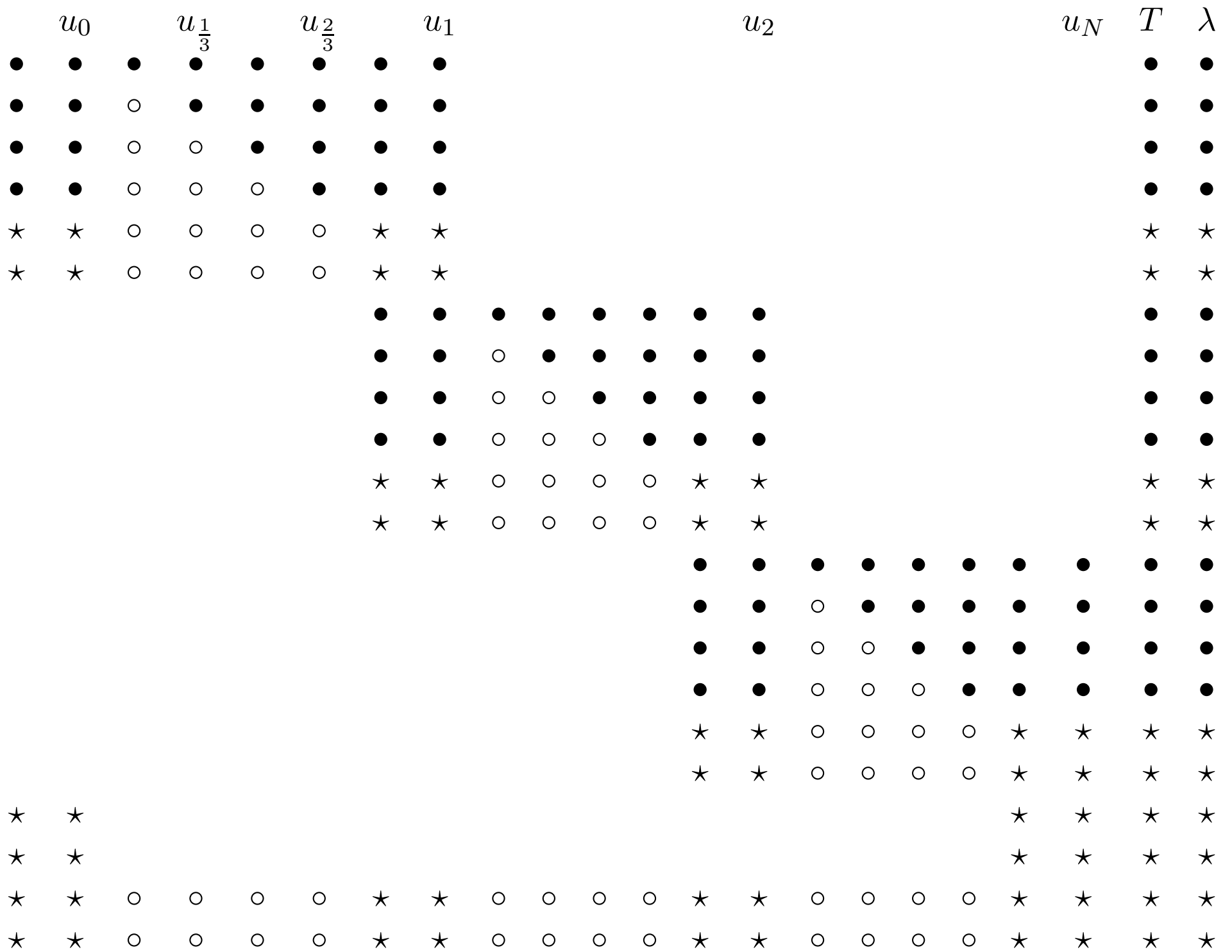- These operations can be done in parallel.

Figure 14:

CAPTION FOR FIGURE 14 :

- The matrix from the preceding Figure, except with some entries now marked by a " $\star$ ".

- The $\star$ sub-system is fully decoupled from the remaining equations.

- The $\star$ sub-system can therefore be solved separately.

- This is known as *"condensation of parameters"*.
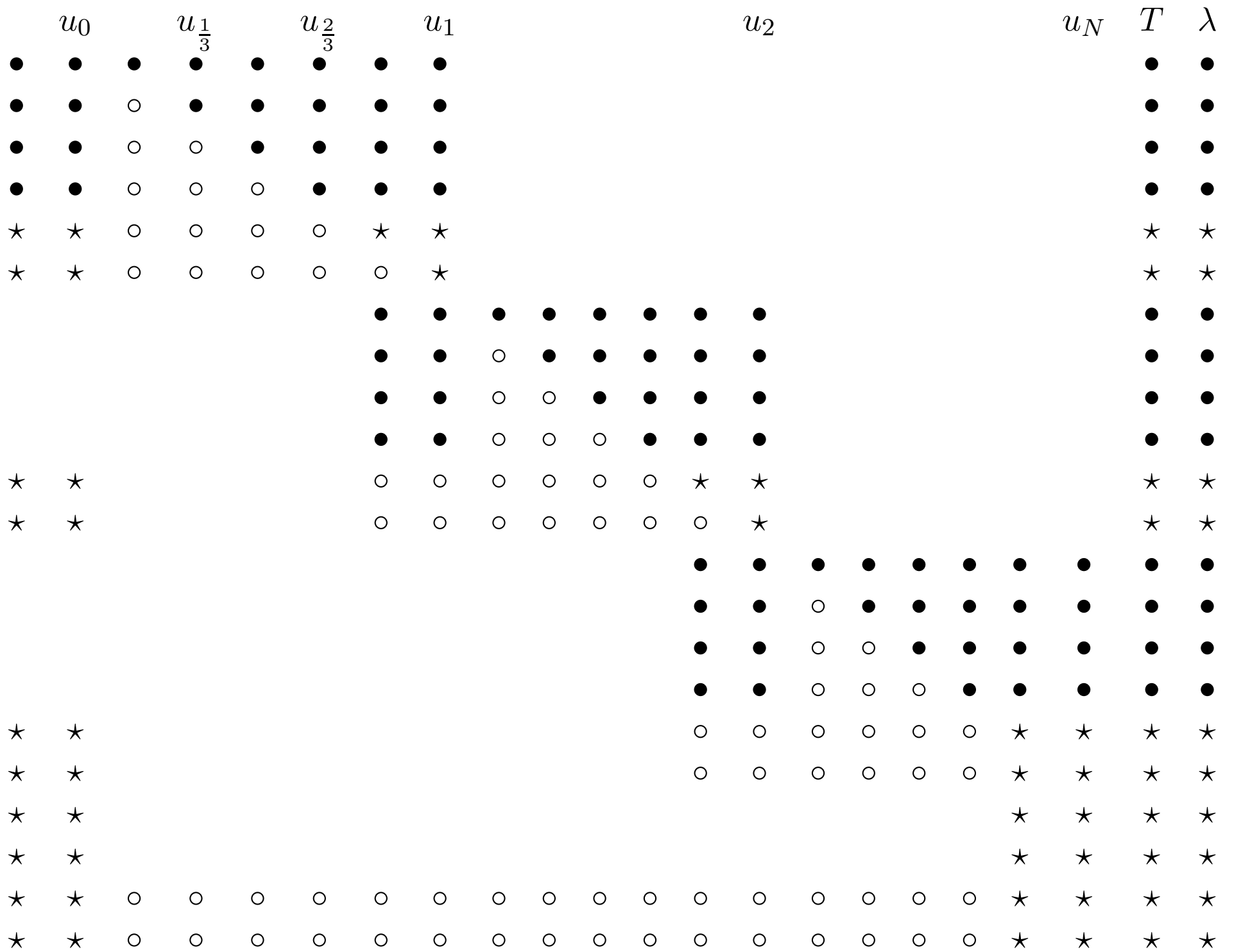
Figure 15:

CAPTION FOR FIGURE 15 :

- The decoupled $\star$ system can be solved by *"nested dissection"*.

- Nested dissection eliminates some of the $\star$'s .

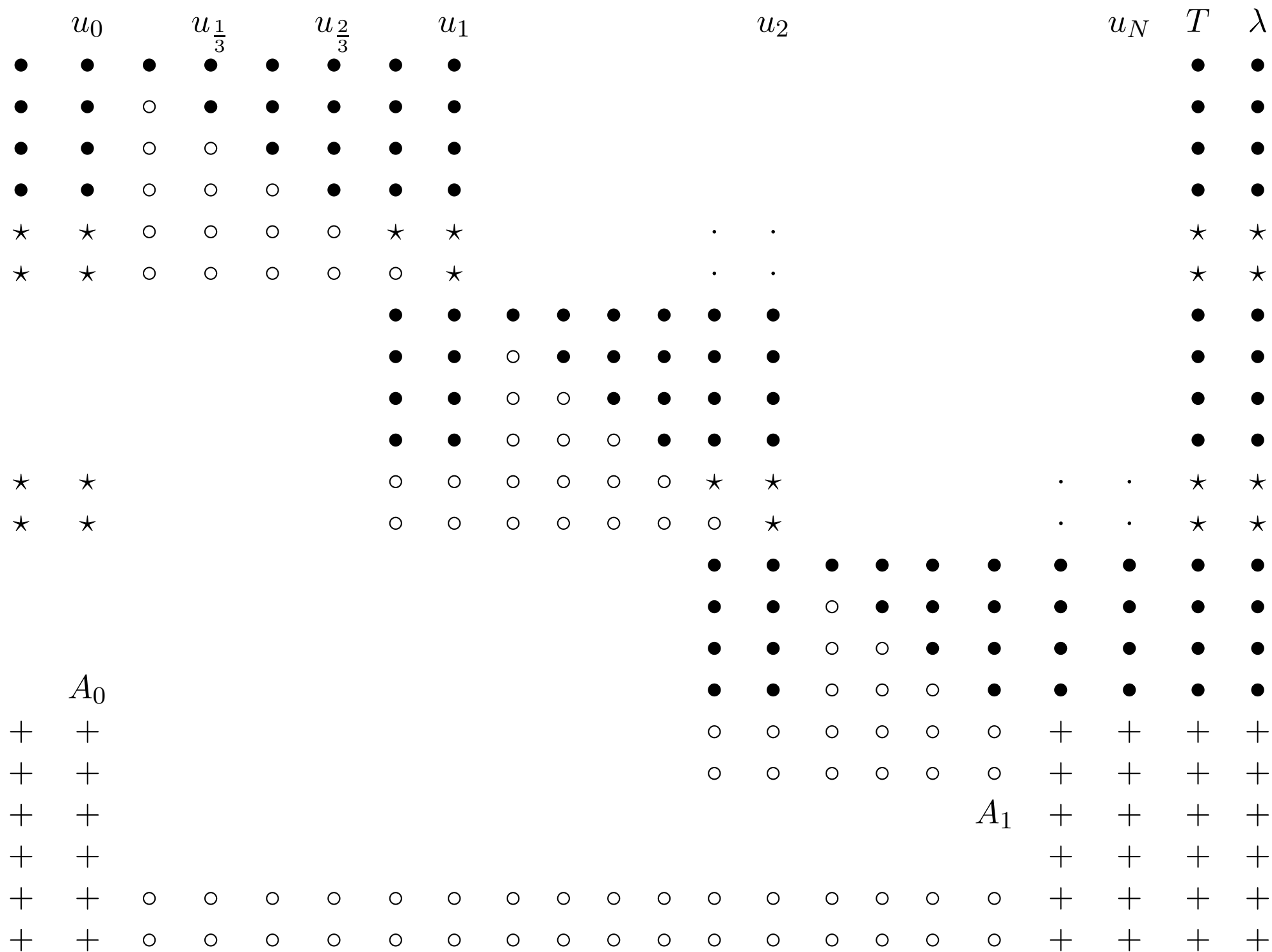- Nested dissection eliminates also introduces some new *"fill-in"*.

Figure 16:

CAPTION FOR FIGURE 16 :

- The same matrix as in the preceding Figure, except with some entries now marked by a " $+$ " .

- The $+$ sub-system is decoupled from the other equations, and can therefore be solved separately.

- For periodic solutions, the Floquet Multipliers are the eigenvalues of the matrix $-A_1^{-1} A_0$.

Computing Periodic Solutions

Stable and unstable periodic solutions can be computed very effectively using a boundary value approach, which also determines the period very accurately, and allows the accurate detection of bifurcation points, including folds, branch points, period-doubling bifurcations, and bifurcations to invariant tori.

The BVP Approach.

Consider

$$u'(t) \ = \ f(\, u(t) \, , \, \lambda \,) \, , \qquad u(\cdot) \, , \, f(\cdot) \in \mathrm{R}^n \, , \qquad \lambda \in \mathrm{R} \, .$$

Fix the interval of periodicity by the transformation

$$t \ \to \ \frac{t}{T} \ .$$

Then the equation becomes

$$\boxed{u'(t) \ = \ T \, f(\, u(t) \, , \, \lambda \,)} \, , \qquad u(\cdot) \, , \, f(\cdot) \in \mathrm{R}^n \, , \qquad T \, , \, \lambda \in \mathrm{R} \, . \qquad (1)$$

and we seek solutions of period 1 , *i.e.,*

$$\boxed{u(0) \ = \ u(1)} \, . \qquad\qquad (2)$$

Note that the period T is one of the unknowns.

Assume that we have computed

$$(\ u_{k-1}(\cdot) \ , \ T_{k-1} \ , \ \lambda_{k-1} \ ) \ ,$$

and we want to compute the next solution

$$(\ u_k(\cdot) \ , \ T_k \ , \ \lambda_k \ ) \ \equiv \ (\ u(\cdot) \ , \ T \ , \ \lambda \ ) \ .$$

The above equations do not uniquely specify u and T .

Specifically, $u(t)$ can be translated freely in time:

If $u(t)$ is a periodic solution, then so is

$$u(t + \sigma) \ ,$$

for any σ .

Thus, a "*phase condition*" is needed.

An example is the Poincaré orthogonality condition

$$(u(0) - u_{k-1}(0))^* \, u'_{k-1}(0) = 0 \, .$$

(Below we derive a numerically more suitable phase condition.)
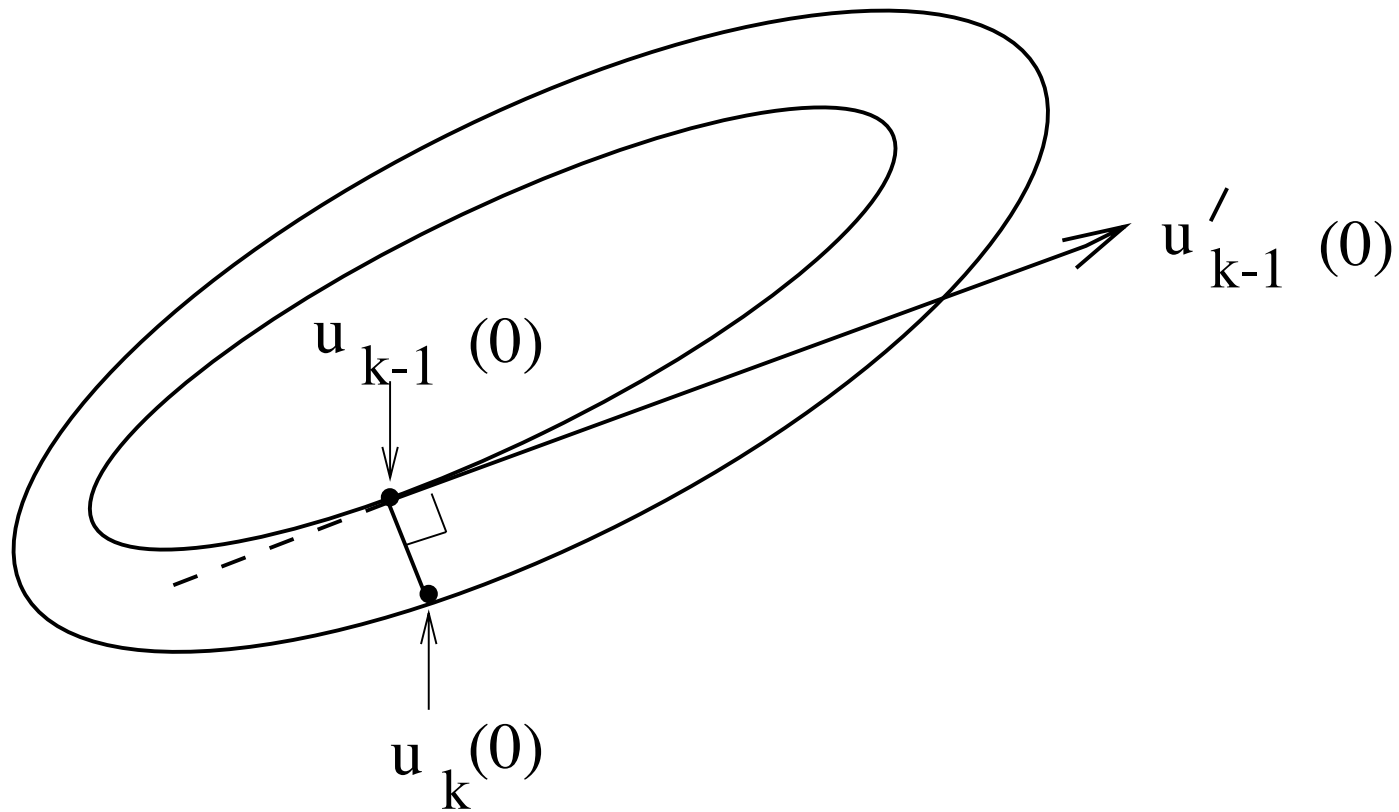
Figure 17: Graphical interpretation of the Poincaré phase condition.

Integral Phase Condition

If $\tilde{u}(t)$ is a solution then so is

$$\tilde{u}(t + \sigma) \ ,$$

for any σ .

We want the solution that minimizes

$$D(\sigma) \ \equiv \ \int_0^1 \| \ \tilde{u}(t + \sigma) \ - \ u_{k-1}(t) \ \|_2^2 \ dt \ .$$

The optimal solution

$$\tilde{u}(t + \hat{\sigma}) \ ,$$

must satisfy the necessary condition

$$D'(\hat{\sigma}) \ = \ 0 \ .$$

Differentiation gives the necessary condition

$$\int_0^1 (\ \tilde{u}(t+\hat{\sigma})\ -\ u_{k-1}(t)\ )^*\ \tilde{u}'(t+\hat{\sigma})\ dt\ =\ 0\ .$$

Writing

$$u(t)\ \equiv\ \tilde{u}(t+\hat{\sigma})\ ,$$

gives

$$\int_0^1 (\ u(t)\ -\ u_{k-1}(t)\ )^*\ u'(t)\ dt\ =\ 0\ .$$

Integration by parts, using periodicity, gives

$$\boxed{\int_0^1\ u(t)^*\ u'_{k-1}(t)\ dt\ =\ 0}\ . \tag{3}$$

This is the *integral phase condition.*

Pseudo-Arclength Continuation

In practice we use pseudo-arclength continuation (see Section) to follow a family of periodic solutions.

This allows calculation past folds along a family of periodic solutions.

The pseudo-arclength equation is

$$\boxed{\int_0^1 (u(t) - u_{k-1}(t))^* \dot{u}_{k-1}(t) \ dt \ + \ (T - T_{k-1})\dot{T}_{k-1} \ + \ (\lambda - \lambda_{k-1})\dot{\lambda}_{k-1} = \Delta s} .$$

$$(4)$$

Equations (1-4) are used in AUTO for continuing periodic solutions.

EXAMPLE.   Consider the equations

$$
\begin{cases}
u_1' & = & -\lambda u_1 & - & u_2 \; , \\
\\
u_2' & = & u_1 \, (1 - u_1) \; .
\end{cases}
\tag{5}
$$

- Note that $u = 0$ is a stationary solution for all λ .

- There is a "vertical" Hopf bifurcation from $u = 0$ at $\lambda = 0$.

- The family ends in an orbit that is *homoclinic* to $(u_1, u_2) = (1, 0)$.

- The terminating orbit has infinite period.

DEMO.   Use AUTO demo `phs` to compute the periodic solutions, and plot some orbits versus time.

Observe how the phase condition keeps the "peak" in the same place. (This is very advantageous for discretization methods.)
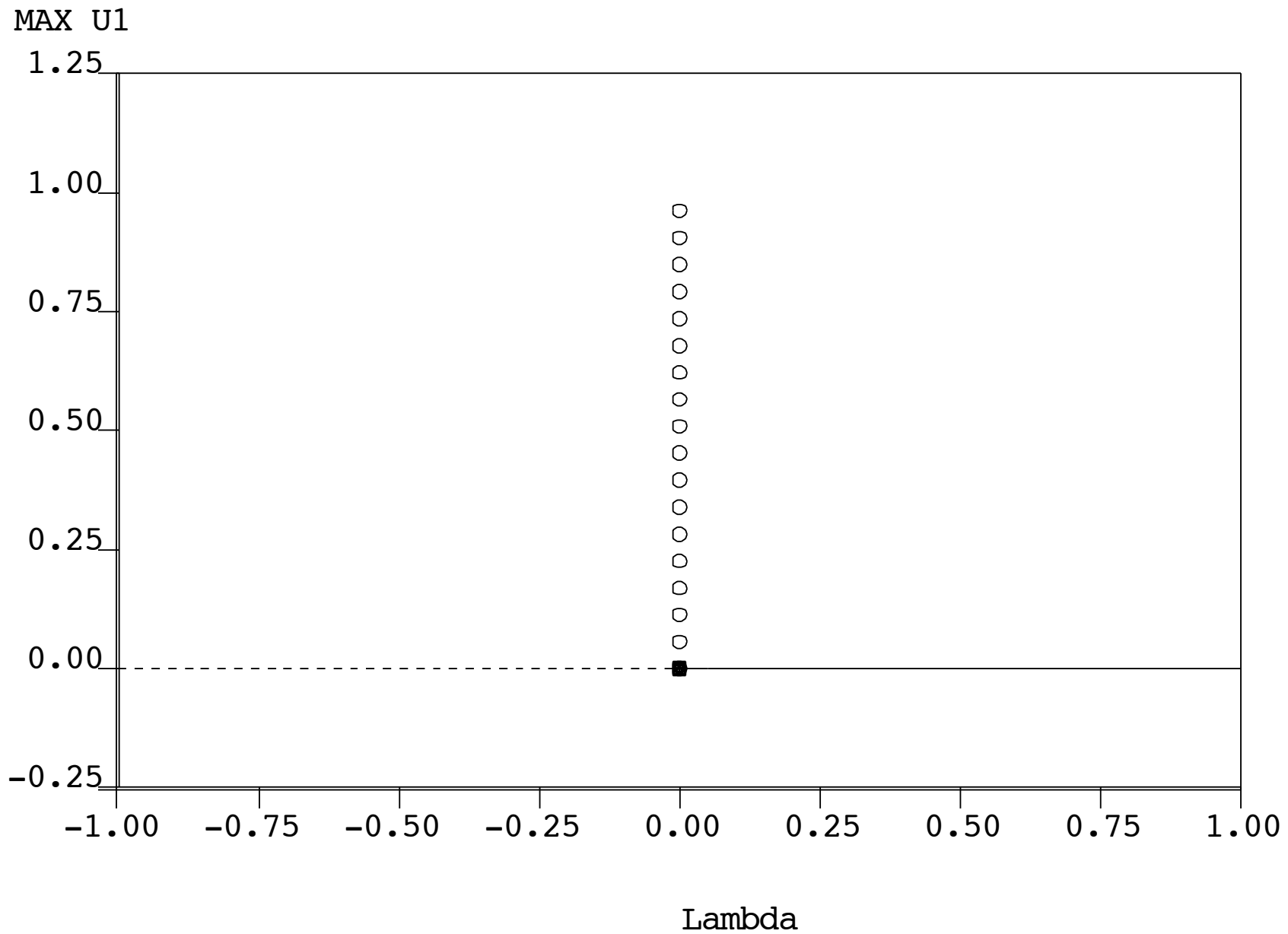
Figure 18: Bifurcation diagram for Equation (5).
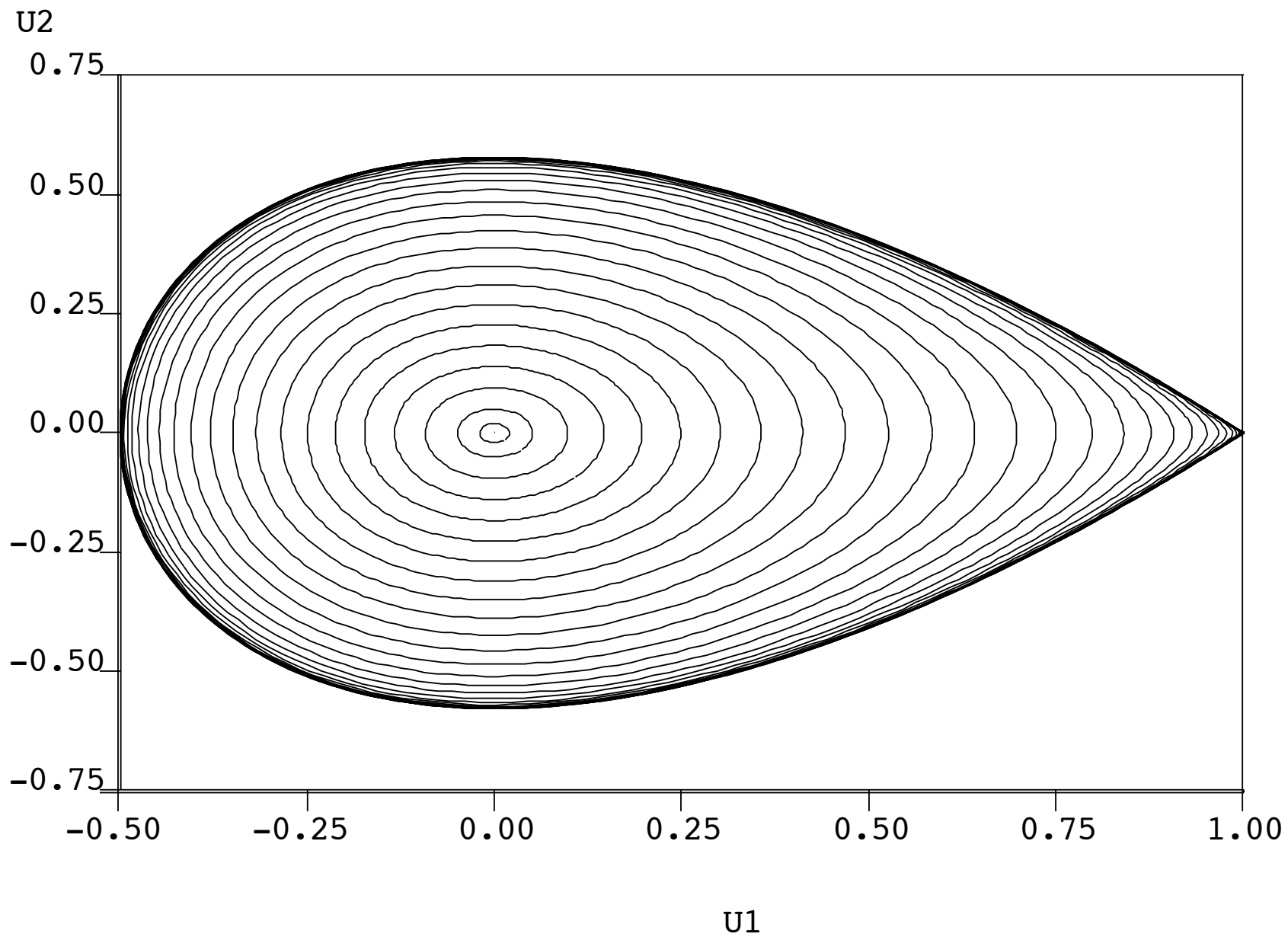
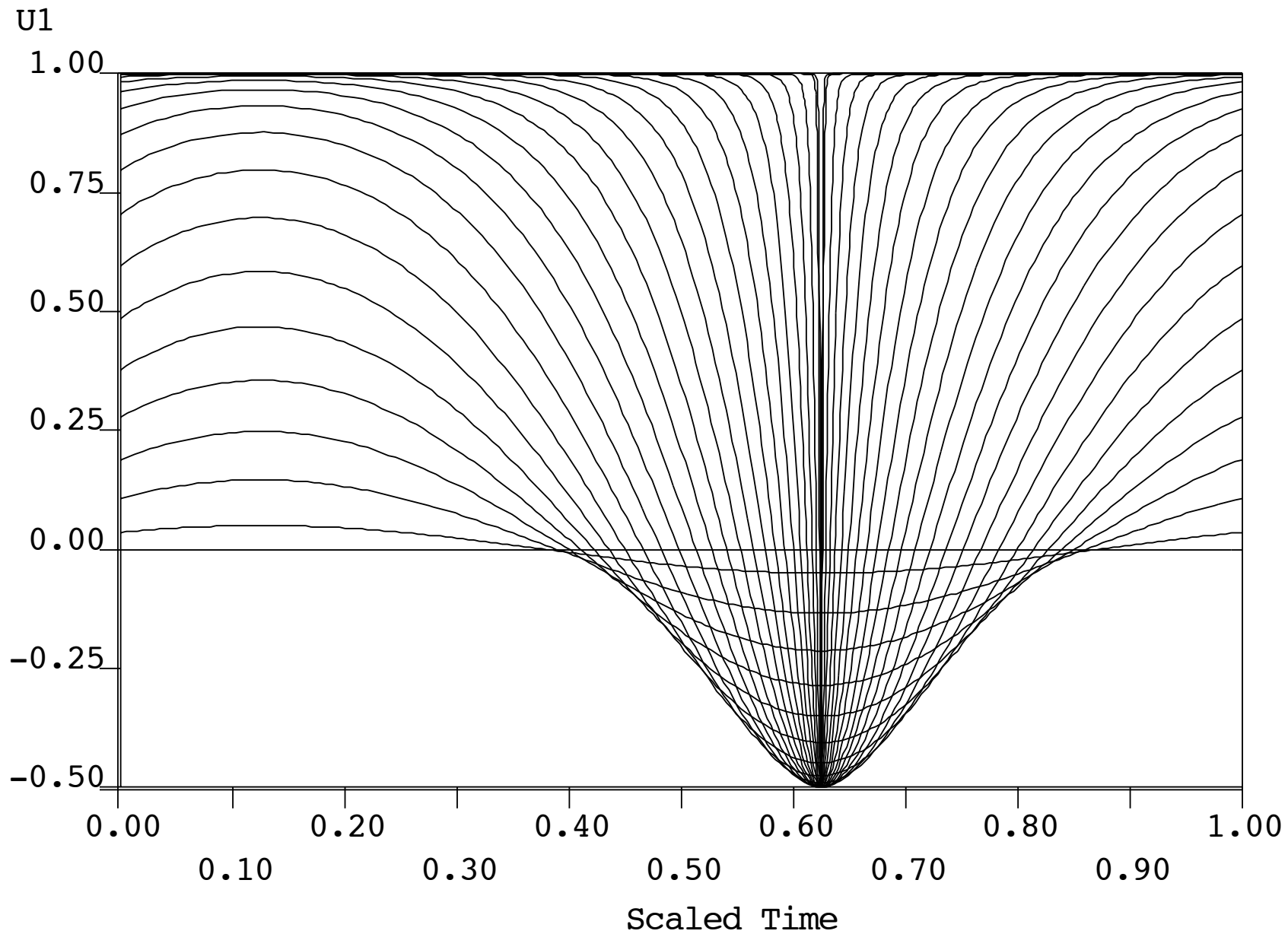Figure 19: A phase plot of some periodic solutions to Equation (5).

Figure 20: u_1 as a function of the scaled time variable t for Equation (5).

Periodic Solutions of a Conservative System

EXAMPLE:

$$u_1' \; = \; - \, u_2 \; ,$$

$$u_2' \; = \; u_1 \, (1 - u_1) \; .$$

PROBLEM:

- This equation has a family of periodic solutions, but no parameter !

- This system has a constant of motion, namely the Hamiltonian

$$H(x_1, x_2) \; = \; - \frac{1}{2} \, u_1^2 \; - \; \frac{1}{2} \, u_2^2 \; + \; \frac{1}{3} \, u_1^3 \; .$$

REMEDY:

Introduce an "unfolding term" with "unfolding parameter" λ :

$$u_1' = -\lambda\, u_1 - u_2 \, ,$$

$$u_2' = u_1\, (1 - u_1) \, .$$

Then there is a "vertical" Hopf bifurcation from the trivial solution at $\lambda = 0$.

In fact, this is our previous example (Equation (5)) !

REMARKS.

- The branch of periodic solutions is "vertical".

- The parameter λ is solved for in each continuation step.

- Upon solving, λ is found to be zero, up to numerical precision.

- One can use "standard" BVP continuation and bifurcation software.

EXAMPLE.   A Singularly-Perturbed BVP.   (AUTO demo `spb`.)

$$\epsilon \, u''(x) \;=\; u(x) \, u'(x) \, (u(x)^2 \;-\; 1) \;+\; u(x) \,.$$

with boundary conditions

$$u(0) \;=\; 3/2 \,, \qquad u(1) \;=\; \gamma \,.$$

Computational formulation

$$u_1' \;=\; u_2 \,,$$

$$u_2' \;=\; \tfrac{\lambda}{\epsilon} \, (\; u_1 \, u_2 \, (u_1^2 \;-\; 1) \;+\; u_1 \;) \,,$$

(6)

with boundary conditions

$$u_1(0) \;=\; 3/2 \,, \qquad u_1(1) \;=\; \gamma \,.$$

COMPUTATIONAL STEPS:

- λ is a homotopy parameter to locate a starting solution.

- In the first run λ varies from 0 to 1 .

- In the second run ϵ is decreased by continuation.

- In the third run $\epsilon = 10^{-3}$, and the solution is continued in γ .

- This third run takes many continuation steps.

2D Stable/Unstable Manifolds

Example : The Lorenz Equations

$$x' = p_3 (y - x) ,$$

$$y' = p_1 x - y - xz , \qquad (7)$$

$$z' = xy - p_2 z .$$

Here

$$p_2 = 8/3 , \qquad p_3 = 10 .$$

while p_1 (normally called ρ) is the bifurcation parameter.

DEMO. Use AUTO demo `lrz` to compute the basic bifurcation diagram.
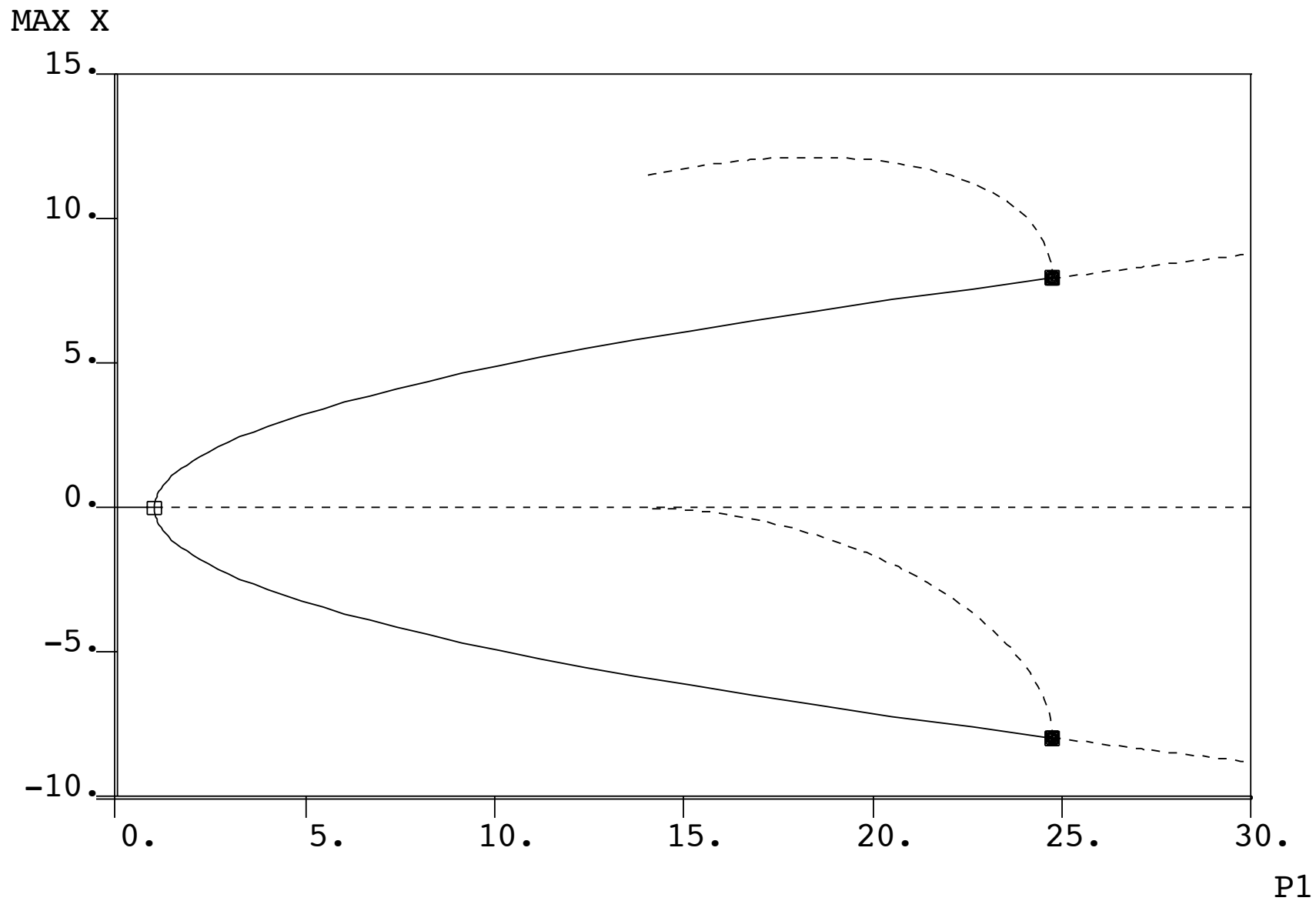
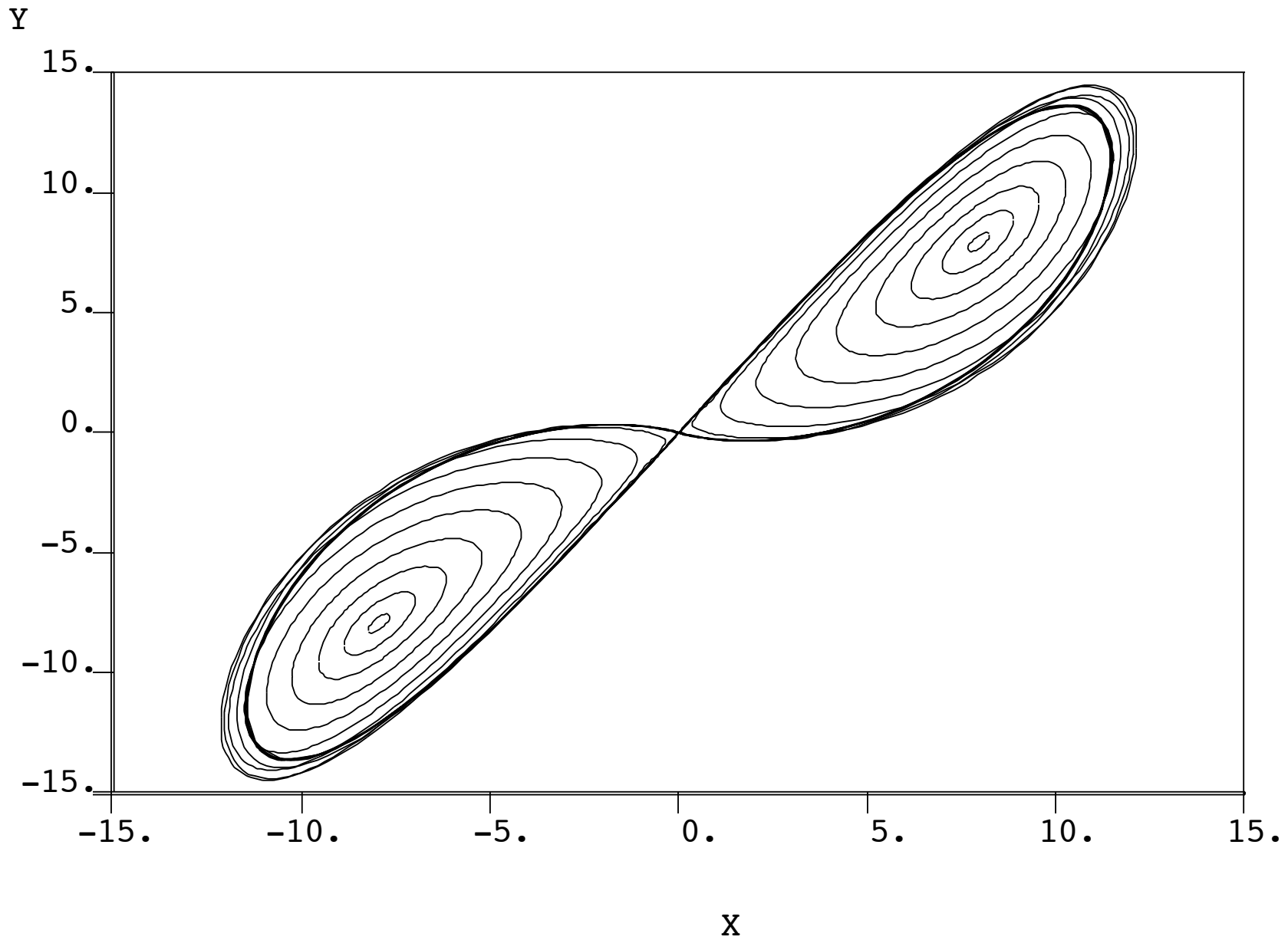Figure 21: Bifurcation diagram of the Lorenz equations.

Figure 22: Periodic orbits of the Lorenz equations.

Now also let $\rho = 28$.

For this parameter value the Lorenz Equations have a "strange attractor".

Let

$$\mathbf{u} = \begin{pmatrix} x \\ y \\ z \end{pmatrix} ,$$

and write the Lorenz equations as

$$\mathbf{u}'(t) = \mathbf{f}(\mathbf{u}(t)) .$$

The origin

$$\mathbf{u}_0 \;=\; \begin{pmatrix} 0 \\ 0 \\ 0 \end{pmatrix} ,$$

is a saddle point, with eigenvalues

$$\mu_1 \;\approx\; -2.66 \;, \qquad \mu_2 \;\approx\; -22.8 \;, \qquad \mu_3 \;\approx\; 11.82 \;,$$

and normalized eigenvectors

$$\mathbf{v}_1 \;, \qquad \mathbf{v}_2 \;, \qquad \mathbf{v}_3 \;.$$

- We want to compute the *stable manifold* of the origin.

The stable manifold of the origin

Compute an initial orbit $\mathbf{u}(t)$, for t from 0 to T (where $T < 0$) , with

$$\mathbf{u}(0) \quad \text{close to the origin} \quad \mathbf{u}_0 \ ,$$

and

$$\mathbf{u}(0) \quad \text{in the eigenspace spanned by} \quad \mathbf{v}_1 \quad \text{and} \quad \mathbf{v}_2 \ ,$$

that is,

$$\mathbf{u}(0) \ = \ \mathbf{u}_0 \ + \ \epsilon \ \left(\frac{\cos(\theta)}{|\mu_1|} \ \mathbf{v}_1 \ - \ \frac{\sin(\theta)}{|\mu_2|} \ \mathbf{v}_2 \ \right) \ ,$$

for, say, $\theta = 0$.

Scale time

$$t \quad \rightarrow \quad \frac{t}{T} \quad,$$

Then the initial orbit satisfies

$$\mathbf{u}'(t) \;=\; T \, \mathbf{f}(\, \mathbf{u}(t) \,) \,, \qquad 0 \le t \le 1 \,,$$

and

$$\mathbf{u}(0) \;=\; \mathbf{u}_0 \;+\; \frac{\epsilon}{|\mu_1|} \, \mathbf{v}_1 \,.$$

The initial orbit has length

$$L \;=\; T \, \int_0^1 \, \| \, \mathbf{f}(\mathbf{u}(s)) \, \| \; ds \,.$$

Thus the initial orbit is a solution of the equation

$$F(X) \ = \ 0 \, ,$$

where

$$X \ = \ (\ \mathbf{u}(\cdot) \, , \ \theta \, , \ T \ ) \, , \qquad \text{(for given } \ L \ \text{ and } \ \epsilon) \, ,$$

and where

$$F(X) \ \equiv \ \begin{cases} \ \mathbf{u}'(t) - T \ \mathbf{f}(\mathbf{u}(t)) \\[2ex] \ \mathbf{u}(0) \ - \ \mathbf{u}_0 \ - \ \epsilon \ \left(\frac{\cos(\theta)}{|\mu_1|} \ \mathbf{v}_1 \ - \ \frac{\sin(\theta)}{|\mu_2|} \ \mathbf{v}_2 \ \right) \\[2ex] \ T \ \int_0^1 \ \| \ \mathbf{f}(\mathbf{u}) \ \| \ ds \ - \ L \end{cases}$$

Pseudo-arclength continuation:

$$F(X_1) \ = \ 0 \, ,$$

$$(X_1 - X_0)^* \ \dot{X}_0 \ - \ \Delta s \ = \ 0 \, , \qquad (\| \ \dot{X}_0 \ \| \ = \ 1 \,) \, .$$

where, for example,

$$X \ = \ (\ \mathbf{u}(\cdot) \, , \ \theta \, , \ T \ ) \, , \qquad (\text{keeping} \ L \ \text{and} \ \epsilon \ \text{fixed}) \, .$$

NOTE:

- We do not just change the initial point (i.e., the value of θ).

- The continuation stepsize Δs measures the change in X .

- Every continuation step requires solving a "boundary value problem".

DEMO. Use AUTO demo `man` to compute part of the stable manifold.
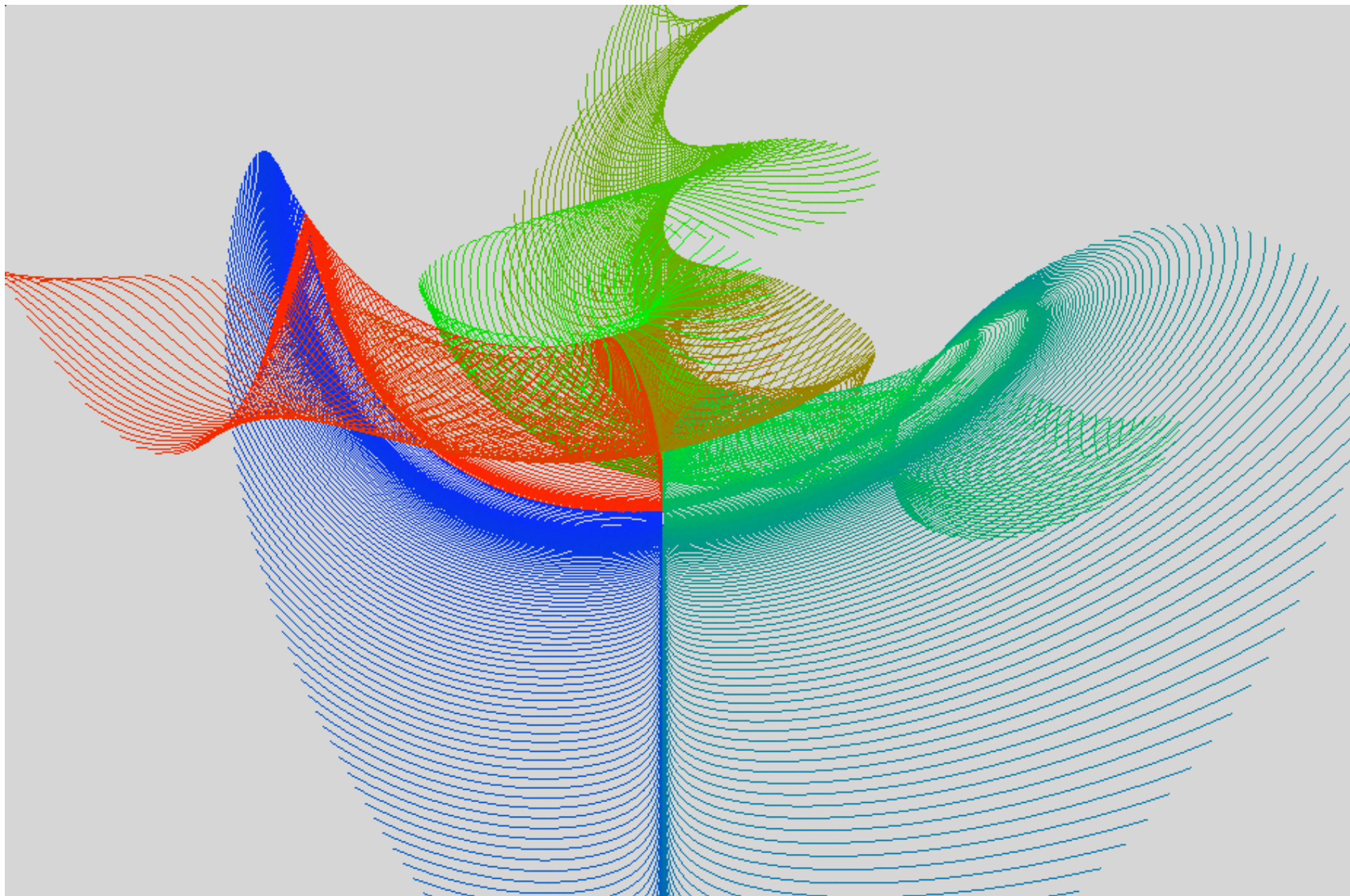
Figure 23: **The stable manifold of the origin in the Lorenz equations.**
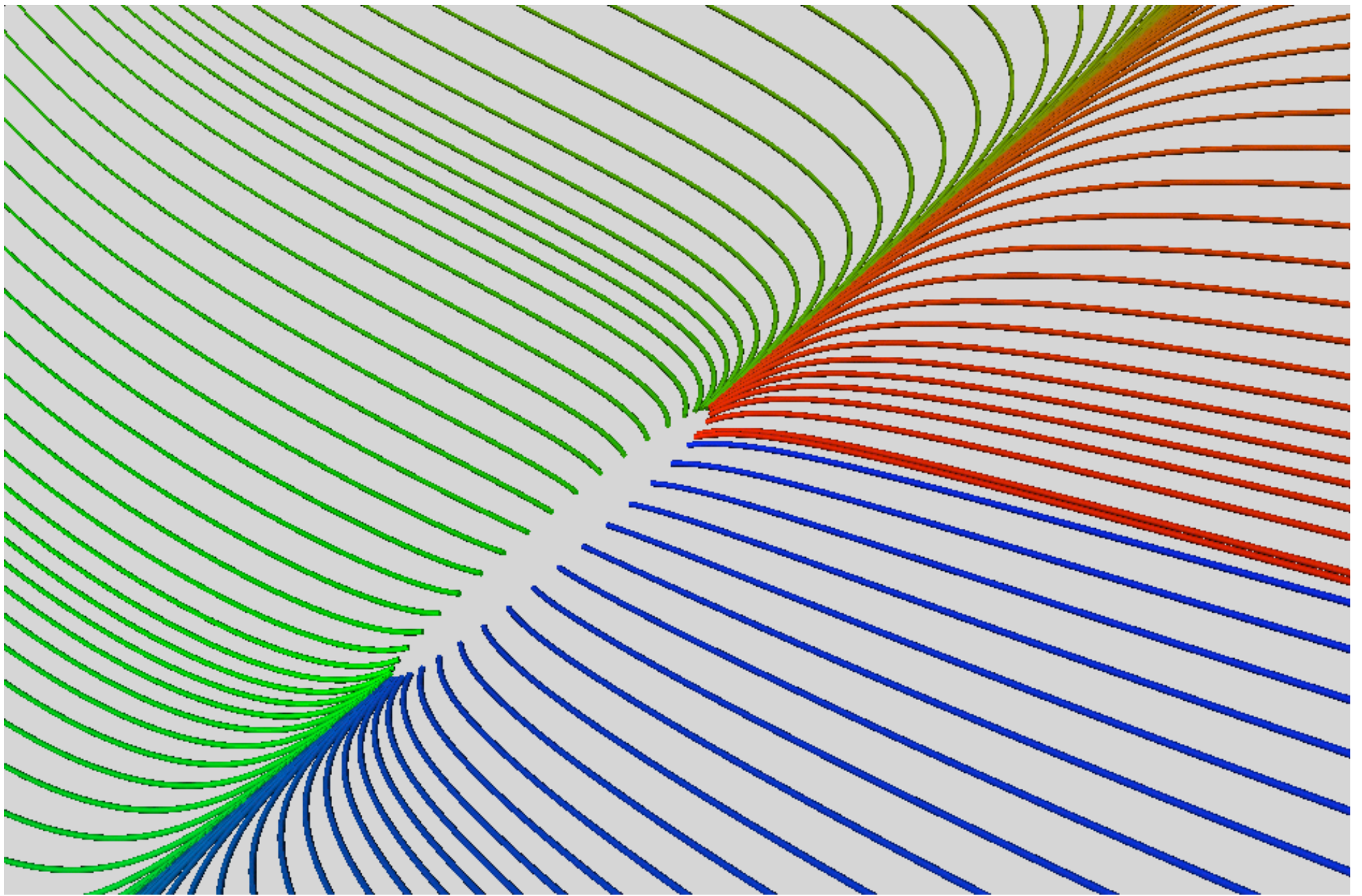
Figure 24: **The stable manifold of the origin in the Lorenz equations.**
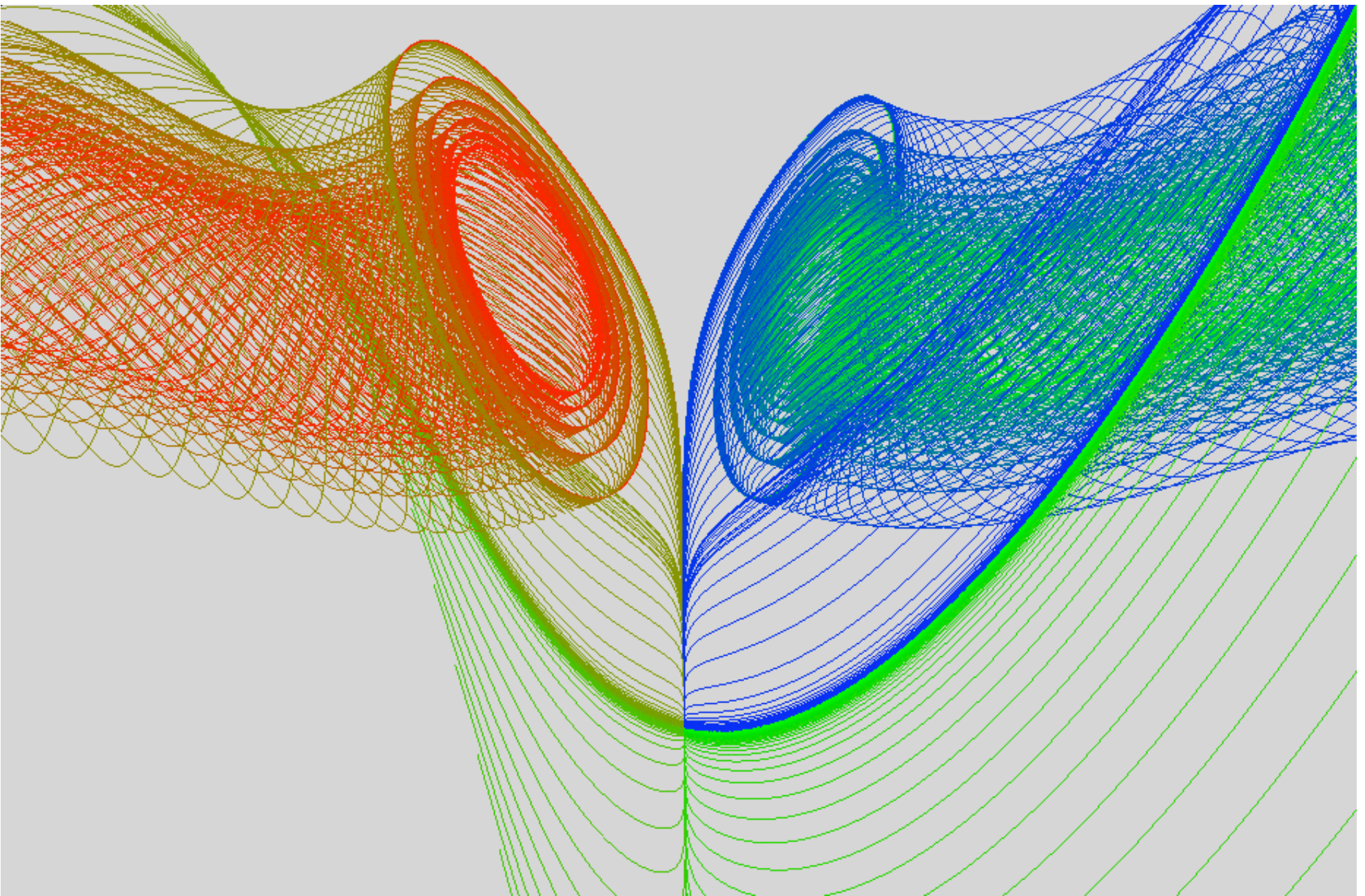
Figure 25: **A section of the Lorenz manifold.**

The unstable manifold of the nonzero equilibria

- One can also compute the 2D *unstable manifold* of the nonzero equilibria.

- The computational set-up is similar, but with complex eigenvalues.

- In this case it is useful to let

$$X = (\mathbf{u}(\cdot) , \epsilon , L) ,$$

  in the continuation procedure, keeping T and θ fixed .

- The stable and unstable manifolds intersect in *heteroclinic connections.*

- These connections correspond to *minima of the arclength L* .

- These connections also correspond to *minima of* $\| \mathbf{u} \|$.
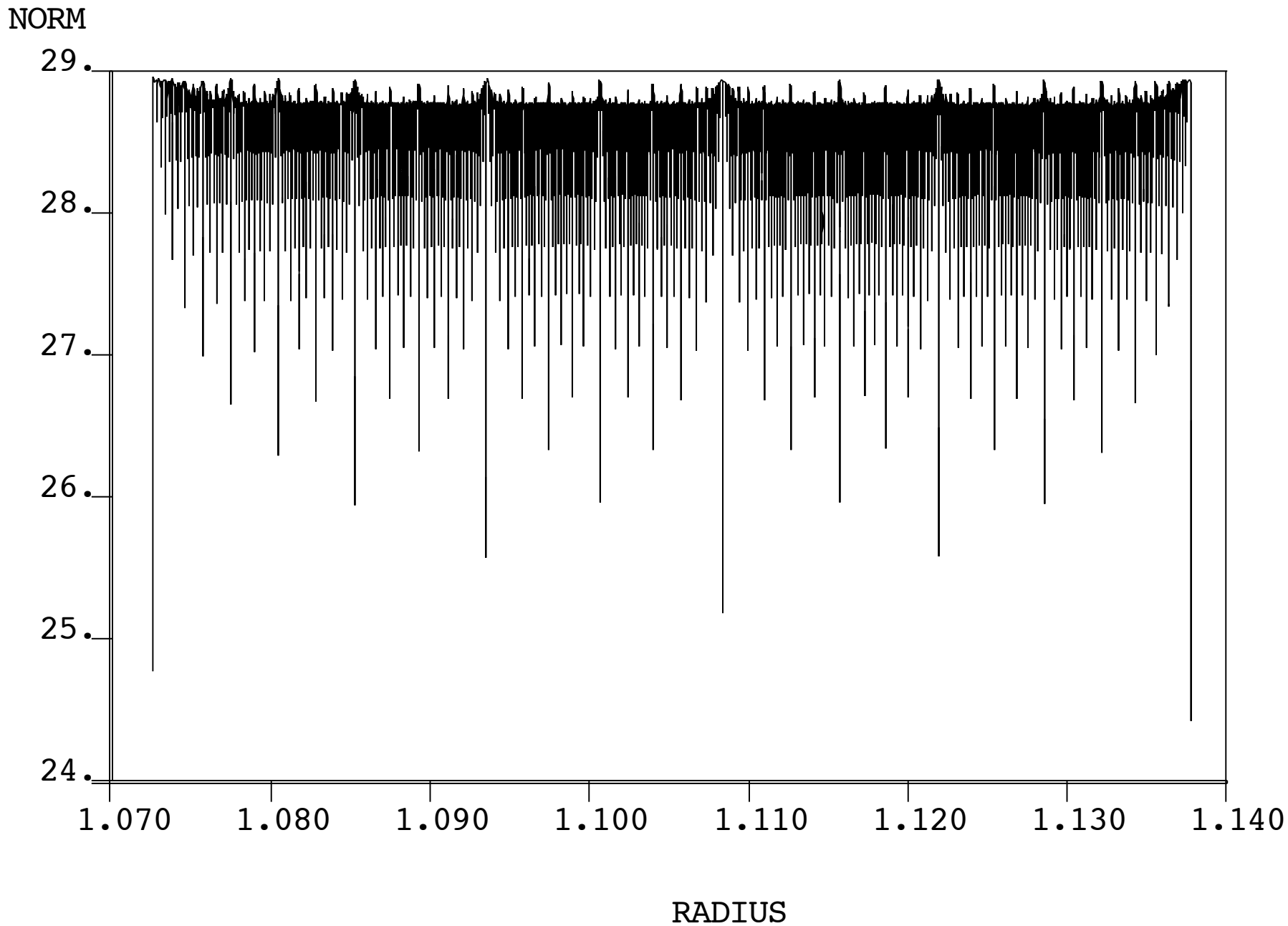
Figure 26: **Representation of the orbits that make up the manifold.**
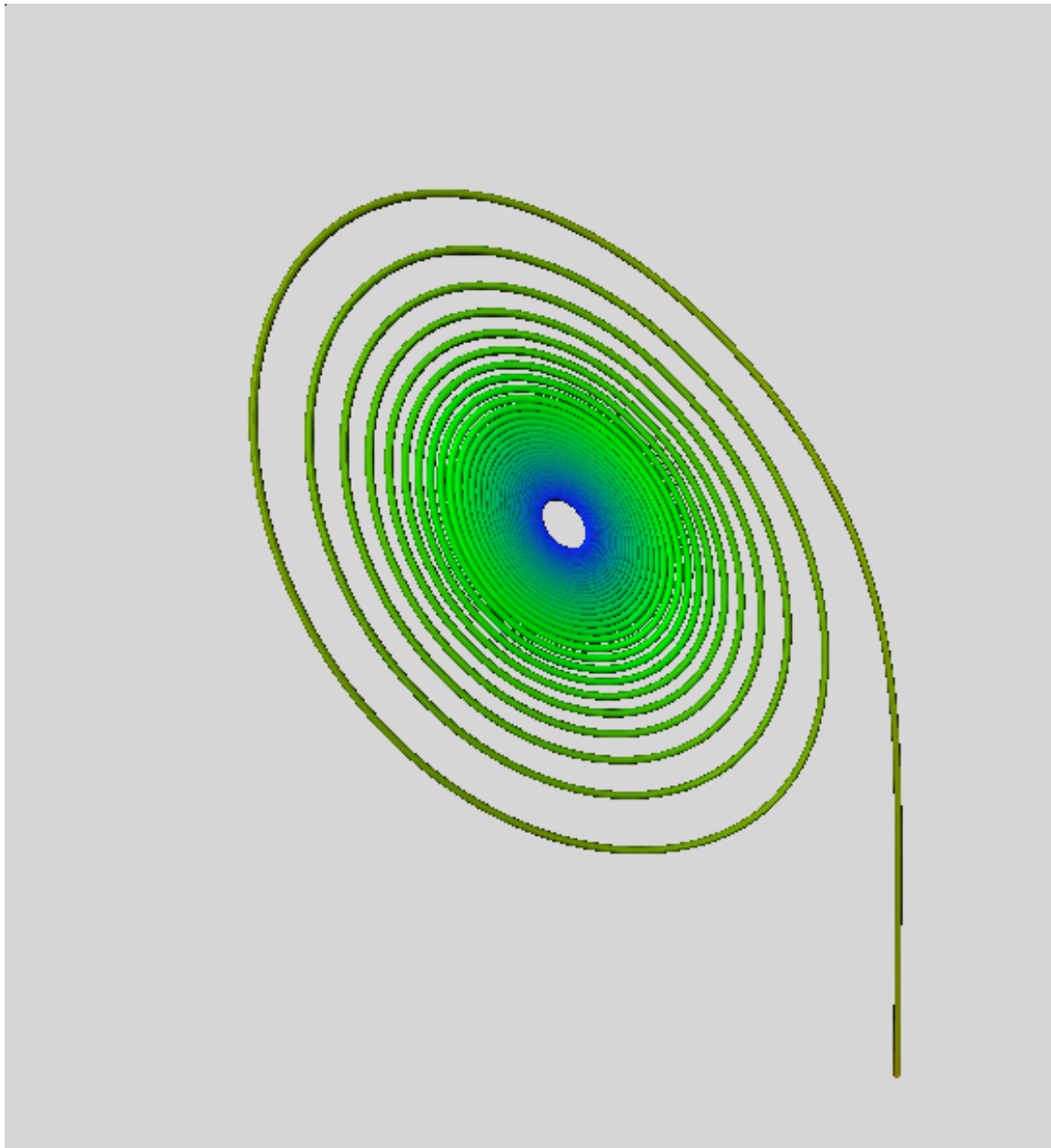
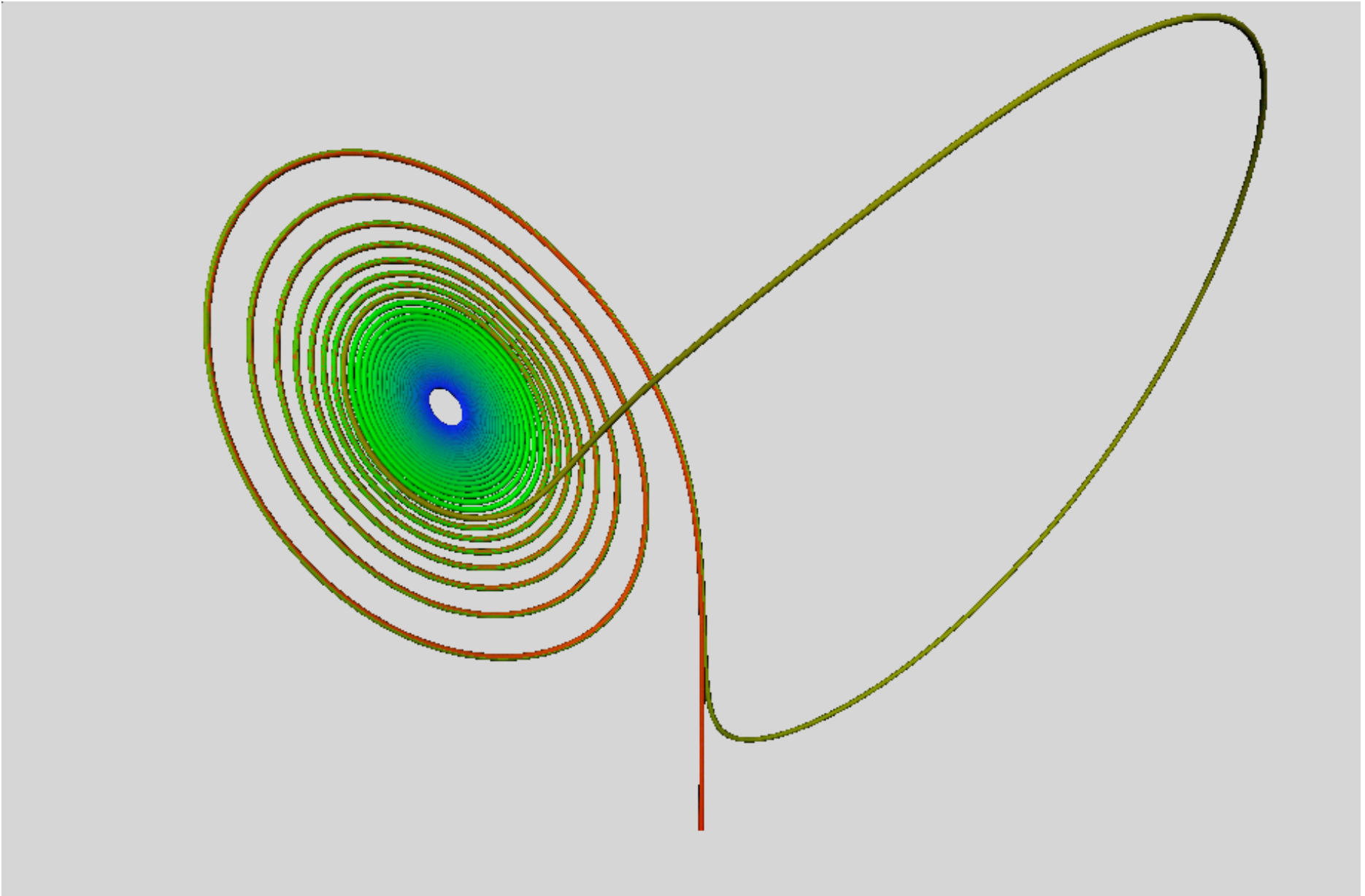Figure 27: **A heteroclinic connection in the Lorenz equations.**

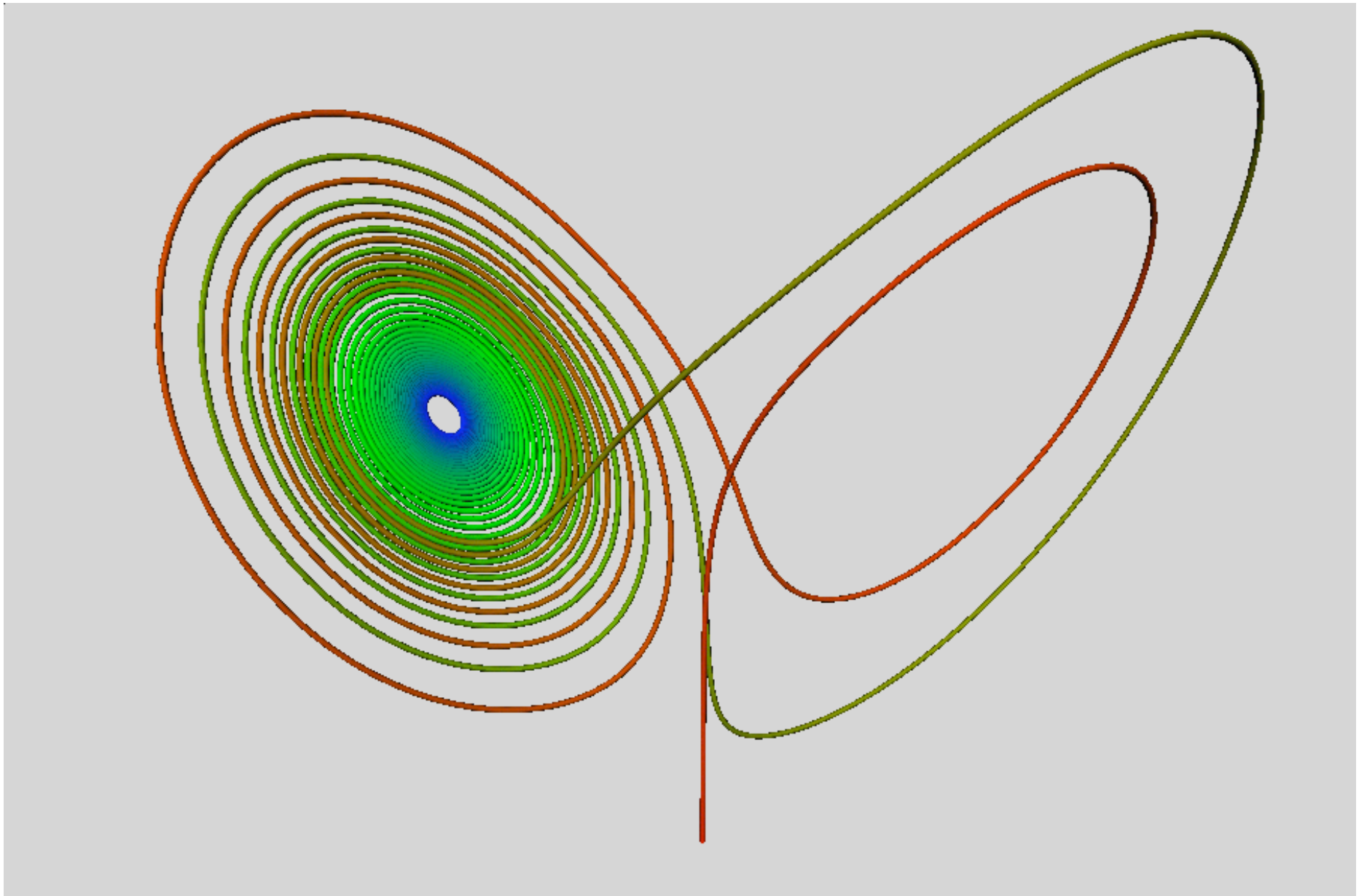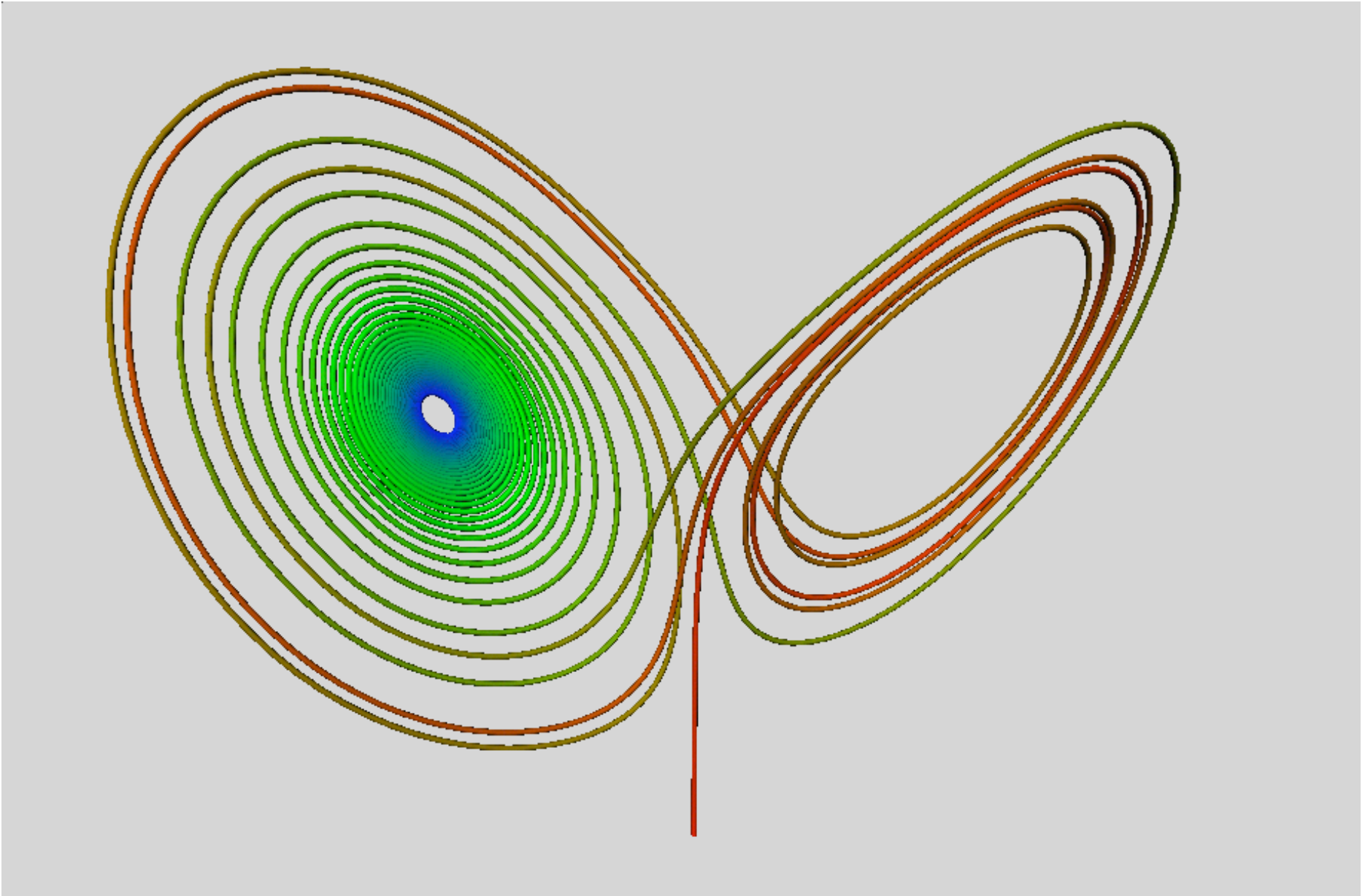Figure 28: **Another heteroclinic connection in the Lorenz equations.**

Figure 29: $\cdots$ **and another** $\cdots$
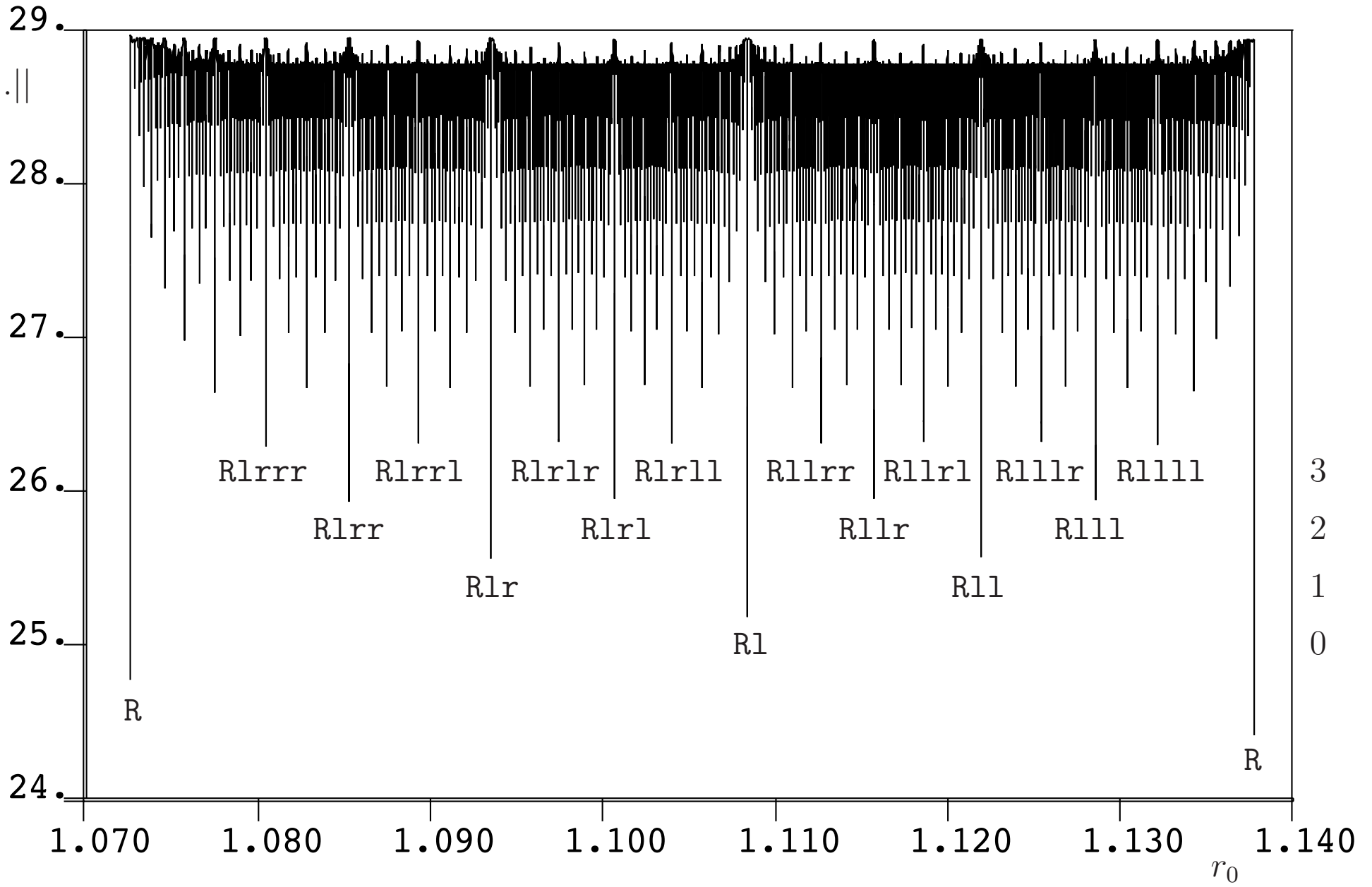
Figure 30: $\cdots$ **and another** $\cdots$

Figure 31: **This continuation calculation located 512 connections!**

REMARKS:

- The heteroclinic connections have a combinatorial structure.

- We can also continue each heteroclinic connection as ρ varies.

- They spawns homoclinic orbits, having their own combinatorial structure.

- These results[*] may shed some light on the Lorenz attractor as ρ changes.

[*] E. J. Doedel, B. Krauskopf, H. M. Osinga, Global bifurcations of the Lorenz model, in preparation.